



Technical University of Crete

Department of Electronic and

Computer Engineering

Graduation Thesis

Modeling and Simulation of an autonomous Photovoltaic/Fuel Cell Hybrid System

by

Ampatzis Michail

A.M. : 2002030030

Supervisor: Dr G. Stavrakakis

Committee: Dr K. Kalaitzakis

Dr D. Kolokotsa

Chania, April 2009

Acknowledgements

I would like to first acknowledge my advisor, Dr Stavrakakis, for his support, advice, enthusiasm and useful information throughout my graduate program. His courses on electrical engineering and renewable energy sources were my motivation for working on this particular thesis. I would also like to express my sincere appreciation for the other members of my thesis committee, Dr Kalaitzakis and Dr Kolokotsa, for their review of my work and the feedback they provided.

A special word of thanks to my parents for their constant, continuous support and encouragement throughout the whole duration of my studies, from the beginning to the completion of this thesis. Finally, I would also like to thank my friends and colleagues, N. Kallitsis, A. Kirillidis, V. Margariti, G. Mitliagkas, K. Mountakis, G. Skoumas, G. Tsiligiannis and M. Theodoroglakis, for their support, cooperation and for making my studies a pleasant, though tiring experience.

Ampatzis Michail

April 2009

Abstract

The purpose of this thesis is the modeling and simulation of a stand-alone hybrid power system, referred to as “hydrogen Photovoltaic - Fuel Cell (PVFC) hybrid system. A stand-alone power system is an autonomous system that supplies electricity to the user load without being connected to the grid. This kind of decentralized system is frequently located in remote and inaccessible areas, due to the difficulty of the utility grid to reach these areas. It consists of a photovoltaic generator, a proton-exchange membrane fuel cell (PEM) unit, an electrolyser unit and a battery. The system is intended to be an environmentally friendly solution since it tries maximizing the use of solar energy. The photovoltaic generator is the main energy source of the system, but it cannot provide enough power to satisfy the load during night hours, or under inappropriate weather conditions. Thus, a fuel cell generator unit is used for satisfying the energy needs when the photovoltaic generator can't. This fuel cell uses pure hydrogen as a fuel, taken from a high pressure storage tank. This hydrogen is not produced by fossil fuels, but from an electrolyser which is fed with the excess energy the photovoltaic generator may produce during daytime. A battery is used as back-up energy storage, and also for ensuring the continuous voltage regulation of the system. The system is sustainable and environmental friendly, as there are no emissions, low noise and there is no connection with the grid.

The location of this stand-alone power system is in Chania, Crete. This location is characterized by its high solar radiation and temperatures, thus having ideal conditions for photovoltaic power generation. Also Crete has many remote and rural areas, with low population density, so this system can be an efficient solution to the problem of electrical energy for these areas. Of course, a lot of progress has to be made in the field of fuel cell mostly, as the cost of this technology nowadays is not attractive to the consumer.

For the simulation of the system Matlab/Simulink was used, mostly because of previous experience with this particular program. The main conclusion in this work is that the simulation of the system under study could successfully be used for visualization of the actual operation of such a system, under the conditions of the location referenced to above. It should also be noted that the Simulink implementation was designed to be easy to parameterize, so different system configurations or different conditions can be examined. The system presented very good behavior under the tested conditions, but the lack of low-cost components cannot make it a popular choice for electricity generation yet. But it should become popular in the future, after a lot of research, both on the photovoltaic and fuel cell power generation fields, and cheaper and more efficient materials have been available.

Keywords: Stand-alone power system, Photovoltaic generation, Proton-exchange membrane Fuel Cell, Electrolyser, Hydrogen storage tank

TABLE OF CONTENTS

1. Introduction.....	9
1.1 Motivation.....	9
1.2 Objectives of the study.....	10
1.3 Outline of thesis.....	11
2. System Overview and Control Strategy.....	12
2.1 Photovoltaic Generation.....	13
2.1.1 General description of a photovoltaic cell.....	13
2.1.2 Sources of loss in a photovoltaic generator.....	14
2.1.3 Maximum power point tracker.....	15
2.2 Hydrogen Energy System and Components.....	15
2.2.1 Electrolyser.....	15
2.2.2 Hydrogen storage.....	17
2.2.2.1 Compressed gaseous hydrogen storage.....	17
2.2.2.2 Liquid hydrogen storage.....	18
2.2.2.3 Metal hydrides storage.....	18
2.3 Control Strategy.....	19
2.4 Conclusion.....	21
3. PV Generator.....	22
3.1 PV Cell.....	22
3.1.1 One-diode model.....	22
3.1.2 Two- diode model.....	24
3.1.2.1 Series Resistance.....	24
3.1.2.2 Parallel Resistance.....	24
3.1.2.3 Recombination.....	24
3.2 PV Module.....	25
3.3 Simulink Implementation of the PV Generator.....	28
3.3.1 PV generator model.....	28
3.3.2 PV cell model.....	32
4. Fuel Cell.....	35
4.1 Introduction.....	35
4.2 Fuel Cell Types.....	37
4.2.1 AFC.....	38
4.2.2 PAFC.....	39
4.2.3 MCFC.....	39
4.2.4 SOFC.....	40
4.3 PEMFC.....	41
4.3.1 Polymer electrolyte membrane.....	42

4.3.2	Catalyst.....	42
4.3.3	Gas diffusion layer.....	43
4.3.4	Water management.....	43
4.4	Mathematical Modeling of PEMFC.....	44
4.4.1	Energy and EMF of the PMFC.....	44
4.4.2	Nernst equation.....	46
4.4.3	Efficiency of PEM fuel cell model.....	47
4.4.4	Hydrogen and fuel cell consumption.....	48
4.4.5	Losses.....	49
4.4.5.1	Activation losses.....	49
4.4.5.2	Fuel crossover and internal currents.....	51
4.4.5.3	Ohmic losses.....	51
4.4.5.4	Concentration losses.....	51
4.5	Simulink Model of PEMFC.....	52
4.5.1	Fuel cell stack.....	53
4.5.2	Fuel Cell.....	54
4.5.2.1	Operating pressure in the fuel cell stack.....	55
4.5.2.2	Nernst equation.....	58
4.5.2.3	Losses.....	59
4.5.3	Electrolyser.....	60
4.5.4	Storage.....	61
5.	Simulation Results.....	63
5.1	Data.....	63
5.2	System Performance.....	67
5.2.1	Winter day.....	67
5.2.2	Spring day.....	72
5.2.3	Summer day.....	77
5.2.4	Special cases.....	83
6.	Conclusions and recommendations.....	88
6.1	Modeling of PVFC Hybrid System Components.....	88
6.1.1	PV generator.....	88
6.1.2	Hydrogen energy system.....	88
6.1.3	Overall operation of hydrogen PVFC system.....	88
6.2	Recommendations for future work.....	88
7.	References.....	90
	Appendix.....	92
	Table of figures.....	92
	List of tables.....	95
	Matlab code for estimation of PV module current.....	96
	Datasheet for fuel cell unit.....	97

Chapter 1-Introduction

1.1 – Motivation

The conventional fossil fuel energy sources such as petroleum, natural gas and coal, which meet most of the world's energy demand today, are being depleted rapidly. Also, their combustion products are causing global problems such as the greenhouse effect and pollution, which are posing great danger for our environment and eventually for the entire life on our planet [1]. The renewable energy sources (solar, wind, geothermal etc) are attracting more attention as an alternative energy. Among the renewable sources, the photovoltaic energy has been widely utilized in low power applications. It is also the most promising candidate for research and development for large scale users as the fabrication of low cost PV devices becomes a reality [2].

Photovoltaic generators which directly convert solar radiation into electricity have a lot of significant advantages such as being inexhaustible and pollution free, silent, with no rotating parts and with size-independent electric conversion efficiency. Because of these advantages they have become a popular choice for smaller or bigger scale applications. With increasing penetration of solar photovoltaic devices, various anti-pollution apparatus can be operated by solar PV power; for example, water purification by electrochemical processing or stopping desert expansion by PV water pumping with tree implantation.

From an operational point of view, a PV power generation experiences large variations in its output power due to intermittent weather conditions. Those phenomena may cause operational problems, such as excessive frequency deviations. In many regions of the world, the fluctuating nature of solar radiation means that purely PV power generators for off-grid applications must be large and thus expensive. One method to overcome this problem is to integrate the photovoltaic plant with other power sources, such as diesel, fuel cell or battery back-up [3], [4], and [5]. The diesel back-up generator for PV power is able to ensure continuous 24 hour power generation, but it has significant disadvantages, such as noise and exhausting polluting gases. In addition, reasonably reliable diesel back-up generators are available only for power range above 5KW, which is too high for a large number of applications. In the middle and small power range this technology cannot be used effectively.

Fuel cell back-up generation is an attractive alternative. In principle, it has very good technical features that make it interesting for stand-alone power supply: high efficiency values, low maintenance, little noise, fast load response, and no production of gases harmful for the environment. At present, the main disadvantages are high cost, low reliability and short service-life. Fortunately, major progress is expected for all these aspects in the next few years, so it makes sense to analyze the potential of using fuel cells in co-ordination with a PV system for both grid-connected or stand-alone power generation. Due to the fast responding capability of the fuel cell power system, a photovoltaic-fuel cell (PVFC) hybrid system may be able to solve the photovoltaic's inherent problem of intermittent power generation [2].

Environmental impacts of fuel cell generated power generation are relatively small in contrast to other fossil fuel power sources. Since chemical reactions inside the fuel cell stack are accomplished by catalysts, it requires a low sulphur-content fuel [6]. Low-emission characteristics of the fuel cell power system may allow some utilities to offset the costs of installing additional emission control equipment. Nevertheless, the positive impact of the fuel cell to the environment is only possible if the hydrogen used as a fuel is produced by a renewable energy source, and not by fossil fuels, which, unfortunately is usually the case today. Therefore, the fuel cell system has great potential for cooperating with a PV generator in a stand-alone power plant, as the one discussed in this thesis.

1.2 – Objectives of the study

It has been well-proven that a photovoltaic power source should be integrated with other power sources, whether used in either a stand-alone or grid-connected system, as it cannot produce power during night hours or under cloudy weather conditions. The system under study in this thesis is a stand-alone hydrogen PVFC power system, which is constituted of a photovoltaic generator, an alkaline water electrolyser, a proton-exchange membrane fuel cell stack, battery as a secondary back-up unit and a tank used for hydrogen storage. This system is intended to be a future competitor of hybrid PV/Diesel systems, especially from an environmental point of view. Hydrogen production in this system, as mentioned before, is produced by electrolyzing water molecules electrically through the electrolyser and is used to produce electricity via the PEM fuel cell stack. This method is a very effective way of producing and using pure hydrogen.

For the study of the system the physical properties of the components were studied, and the corresponding mathematical formulas were derived. Then Matlab/Simulink was used for a dynamic simulation of the system. In general the goals of this thesis are:

- Proper data collecting and/or data synthesizing that describes the system operation and the load profile
- Visualizing and analyzing the system dynamic behavior using power flow trace over middle-term duration, such as one week or one day.
- Creating an accurate simulation system model to predict the real performance of the hydrogen PVFC power system
- Making the parameters of the system as configurable as possible in order the models to be used for a larger variety in applications (mostly different sized applications or components with different datasheets)

It should be noted that some of the control units used in the model of the system, such as the DC/AC converters, were taken by the SimPowerSystems library provided by Simulink.

1.3 – Outline of the thesis

Chapter 1 gives an introduction to the concept of photovoltaic hybrid system and the objectives of the study. Chapter 2 gives an overview of the system, covers background information about the components used and presents the control strategy of the system. Chapter 3 presents the mathematical modeling and Simulink implementation of the fuel cell stack, the electrolyser and the hydrogen tank. Chapter 4 presents the mathematical modeling and Simulink implementation of the PV generator. Chapter 5 presents the simulation results and the discussion about them. Chapter 6 presents the conclusions of this thesis and recommendations for future work.

Chapter 2 – System Overview and Control Strategy

The utilization of intermittent natural energy resources such as solar, wind and hydro energy requires some form of energy storage. The concept of utilizing hydrogen as a substance for storage of energy is shown in Figure 2.1. In this work, a hybrid system based on hydrogen technology is considered. It needs a hydrogen producing unit (electrolyser), a unit for hydrogen storage (tank), and a hydrogen utilizing unit (PEM fuel cell stack). However, the system based on intermittent energy sources and is likely to experience large minutely, hourly and daily fluctuations in energy input. Thus, it should be emphasized that the main purpose of the hydrogen storage system is to store energy over short and long periods of time, i.e., hour to hour and season to season. So, another kind of small energy storage must be used, to provide power in extreme cases, when the PVFC system is unable to respond to the load, and to work continuously in order to be used with the voltage regulator. In addition a control system is required to monitor and guide the operation of the system components. This chapter consists of four sections:

- 1 Photovoltaic generator
- 2 Hydrogen energy system and components
- 3 Battery
- 4 Control Strategy

In this section a brief description of the mentioned components will be given to make the hydrogen PVFC system easy to understand.

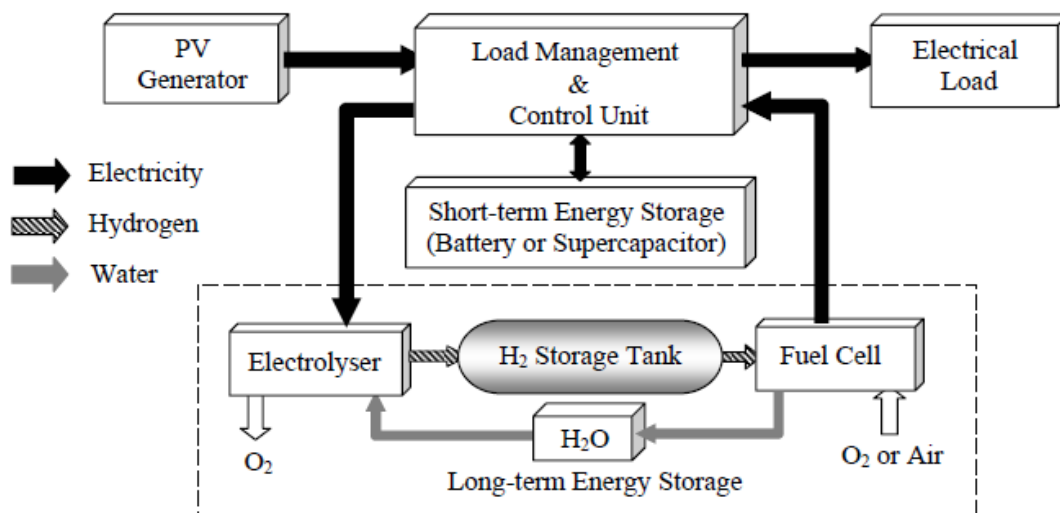


Figure 2.1: Concept of a PVFC hybrid system

2.1 – Photovoltaic generation

In the early 1980s the photovoltaic industries attracted the interest of large energy companies and government agencies. With their capital investment, a tremendous acceleration in PV modules development took place. Today whole product lines are available with PV modules designed to withstand environmental wear for decades. As automation, better designs and improved manufacturing techniques have been applied to PV technology, its price has fallen significantly [7].

2.1.1 – General Description of a photovoltaic cell

Photovoltaic generators convert solar radiation directly into electrical energy. The basic material for almost all photovoltaic cells available in the market, which is highly purified silicon (Si), is obtained from sand or quartz. Basically three types of technology are used in the production of photovoltaic cells: polycrystalline, monocrystalline and amorphous silicon [8]. The crystalline-Si technology is usually used as a reference, or base line, for the solar power generation technology. In general, the status of a photovoltaic cell technology is based on its efficiency and manufacturing cost. The efficiency of a photovoltaic cell is determined by the materials ability to absorb photon energy over a wide range, and on the band gap of the material. Approximate values of the band gap, maximum currents and maximum theoretical efficiencies at room temperatures of some used materials are given in Table 2.1 [9]:

Material	Band gap [eV]	Max. current density [mA/cm ²]	Max. theoretical efficiency [%]
Silicon, Si	1.12	43.4	28
Gallium arsenide, GaAs	1.4	31.8	30
Cadmium telluride, CdTe	1.5	28.5	29
Amorphous silicon, a-Si	1.65	21.7	27

Table 2.1: Band gap, maximum current density and theoretical efficiency of some different semiconductor technologies

Crystalline and polycrystalline silicon are the materials most commonly used in photovoltaic cells. The advantage of silicon cells is primarily the abundance of silicon on Earth. The photovoltaic cell consists of several layers of semiconductor materials with different electronic properties. In a typical polycrystalline cell, the bulk of the material is silicon, doped with a small quantity of boron to give it a positive or p-type character. A thin layer on the front of the cell is doped with phosphorous to give it a negative or n-type character. The interface between these two layers produces an electric field and forms the so-called “cell-junction” [10].,

When the cell is exposed to sunlight, a certain percentage of the incoming photons is absorbed in the region of the junction, freeing electrons in the silicon crystal. If the photons have enough energy, the electrons will be able to overcome the electric field of the junction and to move through the silicon and into an external circuit. The direction of the electrical current is opposite to its direction if the device operates as a diode.

A photovoltaic generator consists of a number of modules, formed by the interconnection of photovoltaic cells, connected together in series and parallel to provide the required voltage and current. Therefore, the performance of the PV generator depends on the modules that comprise the generator and the cells that comprise the modules. The operating point of the generator is defined by the intersection of its I-V characteristics with the load line of the load connected to it [2].

2.1.2 – Sources of loss in a photovoltaic generator

There are five kinds of losses in a PV generator:

- 1 **Reflection losses:** When the incidence angle of the solar radiation differs from the perpendicular direction on the surface of a PV generator, reflection losses occur which will cause an overestimation of the PV yield under field conditions. These losses are reduced by coating the surface with an anti-reflection layer [10].
- 2 **Spectral losses:** The solar radiation is characterized by a wide solar distribution because the air-mass (AM) value changes during the day. The solar radiation contains photons with extremely different energies. Photons with smaller energy than the band gap energy are not absorbed and thus are unused. In case of photons with larger energy than the band gap energy, only the amount of energy that equals to the band gap energy is useful, so the excess energy is dissipated as heat in to the crystal lattice.
- 3 **Mismatch losses:** The I-V characteristics of PV modules from the same type and the same manufacturer can vary from one module to another. According to the information from the suppliers, the MPP (Maximum Power Point) of a module under STC can deviate up to 10% from the datasheet characteristics. By series and parallel connection of the modules in a PV generator, the different I-V characteristics will produce power losses which are called mismatch losses [11].
- 4 **Shadowing losses:** The characteristics of the PV generators are affected by the presence of partial shadowing, especially the value of maximum output power, the fill factor and the efficiency of the PV generator. Therefore, it is very important to choose the suitable site for the PV generator to prevent partial shadowing during the operation of the PV system [12]. The fill factor mentioned before is defined as the ratio of the output power at the maximum power point to the power computed by multiplying the V_{oc} (open-circuit voltage) by the I_{sc} (short-circuit current).
- 5 **External losses:** In a real system, the PV generator output power is not exactly equal to the input power to connected power conditioning unit. In order to calculate this input power, the losses caused by the voltage drop due to cable resistances and the blocking diodes have to be considered. The losses caused by resistance of the connecting cables (Ohmic losses) have to be calculated based on cables length and diameter. This resistance is considered as a series resistance, as it is discussed in the next chapter. In each string that forms the PV generator, blocking diodes are connected in series with these strings. If a short circuit occurs in one or more of these strings, the blocking diodes will prevent the currents to flow from the perfect strings to the faulty strings. During operation there is a voltage drop through each diode of approximately 0.7V. This value has to be subtracted from the output voltage of the PV generator.

2.1.3 – Maximum Power Point Tracker

The position of the maximum power points on the PV generator characteristics depends strongly on the solar radiation and the cell temperature. It is used to adjust the actual operating voltage and current of the PV generator so that the actual power approaches the optimum value as closely as possible. Operation of the PV generator at its MPP involves matching the impedance of the load to that of the generator. For this purpose, an electronic device, usually a power conditioning unit, capable of performing the function of a MPPT has to be connected between the PV generator and the load. Therefore, a tracking of the MPP is only meaningful, if components for processing are available, and the tracking of the working point does not bring additional energy losses and at small additional costs. Many different techniques have been used in order to track maximum power point for generator [13] and [14]. These techniques can be classified either as direct or indirect methods. The direct methods are based on a searching algorithm to determine the maximum of the power curve without interruption of the normal operation of the PV generator. For a certain working point, the corresponding voltage is changed around by a certain increment. Consequently, if the output power becomes larger than the value calculated, then the search direction is maintained for the next step. Otherwise it will be shifted to the opposite direction. The indirect methods use an outside signal to estimate the MPP. Such outside signals may be given by measuring the solar radiation, the module temperature, the short circuit current, or the open circuit voltage of a reference PV cell. A set of physical parameters has to be given, and the MPP set point is derived from the monitored signal.

2.2 – Hydrogen energy system and components

Hydrogen is one of the most promising alternative fuels for the future because it has the capability of storing energy of high quality. Therefore, the hydrogen has been visualized to become the cornerstone of future energy systems based on PV energy and other renewable energy sources. The concept of using hydrogen as an energy carrier in storage and transport has been studied by many scientists from all around the world [15] and [16]. The function of a fuel cell and a fuel cell stack are discussed very thoroughly in Chapter 4. So, in this section the electrolyser and the tank will be discussed.

2.2.1 – Electrolyser

An electrolyser converts electricity into chemical energy which produces hydrogen. Hydrogen can be stored for example into pressure tanks or metal hydrides. Hydrogen can be produced from water electrolysis in several ways such as alkaline, acidic, and solar photo production. Alkaline and acidic water electrolysers are commercially available today.

The function of the alkaline water electrolyser is to decompose water into hydrogen and oxygen and this can be achieved by passing a DC electric current between two electrodes separated by a KOH electrolyte with good ionic conductivity. Water is a very poor ionic conductor and for this reason a conductive electrolyte must be used, so that the reaction can proceed at a technically acceptable cell voltage. The half cell reactions and the overall reaction are:

- Anodic half reaction: $2OH^- \rightarrow \frac{1}{2}O_2 + H_2O + 2e^-$
- Cathodic half reaction: $2H_2O + 2e^- \rightarrow H_2 + 2OH^-$
- Overall reaction: $H_2O \rightarrow H_2 + \frac{1}{2}O_2$

In figure 2.2 a plot of the theoretical and actual voltages for an alkaline water electrolyser cell versus the current density at high and low operating temperatures are shown. The difference between the two I-V curves is mainly due to the temperature dependence of overvoltages.

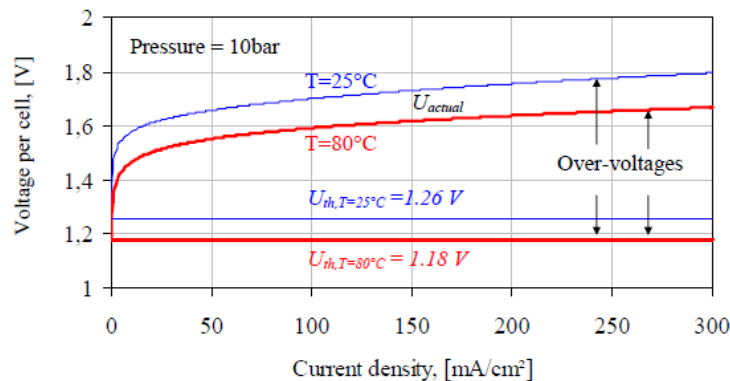


Figure 2.2: I-V curves for an electrolyser cell for low and high temperatures

In our system the electrolyser model is not complex and it consists of 75 cells.

Standard alkaline water electrolyser, which makes use of fossil fuel sources of electricity, is much cheaper than renewable electrolyser, which makes use of solar or wind power sources of electricity. However, the standard alkaline water electrolyser suffers the environmental penalties resulting from fossil fuel burning in power plants, and represents very little progress away from the current energy regime. The capital costs of standard alkaline water electrolyzers range from 300\$/kW to 600\$/kW [17]. For example, a 2MW alkaline water electrolyser with an efficiency of approximately 80% would cost roughly 600\$/kW and the price of hydrogen produced is approximately 20\$/GJ [17]. Although the environmental benefits of the renewable electrolyser far surpass other methods, its use is not recommended in the short-term. Renewable methods of electricity production are themselves a developing technology. The cost of hydrogen production from a renewable electrolysis is simply high to be economical. However, as a long-term goal, this production method is quite promising. The cost of the electrolyser remains decreasing, as component materials continue to be changed and developed.

2.2.2 – Hydrogen Storage

Before discussing some methods of hydrogen storage, the properties and characteristics of hydrogen must be mentioned. Hydrogen is the simplest and most abundant element in the universe. It is clean and pollution free. Some characteristics of hydrogen are:

- It is colourless, odourless and has no taste
- It is the lightest of all elements (molecular weight = 2.016g/mol). Its density is about 14 times less than air (0.08376 kg/m^3 at standard temperature and pressure), it has a very high diffusion rate.
- It is liquid at temperatures below 20.3K at atmospheric pressure. The density as liquid is 70.8 kg/m^3
- It contains the highest energy per unit mass of all fuel cells ($HHV = 141.9 \text{ MJ/kg}$ or 11.89 MJ/m^3 , and $HHV = 111.9 \text{ MJ/kg}$ or 10.043 MJ/m^3). One pound of hydrogen has three times the energy content of one pound of gasoline
- It has a small molecular size, allowing it to leak easily through porous materials than other common gases at equivalent pressures. At the same holes or joints, it leaks about 1.26 to 2.8 times faster than natural gas.
- It is generally non-corrosive and non-reactive with typical container materials.
- It is non-toxic and non-poisonous. In contrast, the combustion products of diesel and other conventional fuels are more toxic from an inhalation standpoint.

When an energy system is totally based on renewable or intermittent power systems, the problem arises that the energy demand pattern cannot be fully fulfilled by online power generation. An energy storage system must be put in between the power generation and the power utilization.

Hydrogen has been proposed as the core medium for solving this problem. Hydrogen is not a primary energy source, but it is utilized as an energy carrier between power generation and power utilization. Power is generated from hydrogen either by conversion in a fuel cell, or by combustion in an internal combustion or turbine engine. Hydrogen can be stored in many basic configurations such as pressurized hydrogen gas, which is the case in the system studied, or liquid hydrogen in tiny micro spheres or in metal hydride compounds. The various storage types have different characteristics. The selection of a specific storage type depends on these characteristics, and mainly on energy density and cost of each type. The different types of hydrogen storage are discussed in the following sections.

2.2.2.1 – Compressed gaseous hydrogen storage

Compressed gaseous hydrogen can be stored in pressure tanks at ambient temperature and 200 up to 700bar pressure. The most common materials used for hydrogen tanks are steel and aluminum. From all storage technologies, the compressed gaseous hydrogen has the longest history and cheapest price. This storage type is suitable for electrolyzers, which can produce hydrogen at high pressures. The theoretical gravimetric energy density of hydrogen can be calculated the molar mass of hydrogen molecule (2.016g/mol) to be 39.4kWh/kg [15]. The actual gravimetric energy density of stored hydrogen

is largely dependent on the material of the container since light materials usually do not tolerate pressure as well as heavier ones. With a traditional steel tank energy density of about 0.45kWh/kg could be achieved, which is equivalent to 1.14% of the weight of stored hydrogen. The material development of tanks has taken a tremendous step with the development of different composites. Therefore, with these composite tanks, the energy density is increased to 4.45kWh/kg, which is equivalent to 11.3% of the weight of stored hydrogen [18]. Compressed gaseous hydrogen can be stored either in aboveground portable or stationary tanks or in different kinds of earth caves. The aboveground hydrogen storage tanks vary in size but are typical in standard pressure. One of the best properties of the aboveground tanks is that they do not leak. The losses of the storage capacity are thus virtually non-existent [19]. Some leaks may occur through connectors but with proper fittings and regulators these leaks could be minimized. The underground caves are an easy and relatively cheap method for large size storage of hydrogen. The pressure in earth caves varies between 80-160bar and thus the volumetric energy density is about 250-465kWh/m³ [15]. The losses caused by the leaks in earth caves are about 13% of the total volume per year.

2.2.2.2 – Liquid hydrogen storage

Liquid hydrogen has been used as a fuel in space technology for several years [15]. It is light and has less potential risks in terms of storage pressure compared with the compressed gas. The hydrogen liquefies to a colourless liquid at –253°C (20.3K) and thus the storage tanks require sophisticated insulation techniques. Liquid hydrogen is stored in standing or lying tanks of 3-75m³ under a pressure of 12bar [20]. The energy needed to liquefy the hydrogen is about 20 to 30% of the energy content of hydrogen. This is one of the largest problems concerning the use of liquid hydrogen. However, this loss of energy is quite compensated with high energy density of liquid hydrogen. An amount of 1%/day of the stored hydrogen must be evaporated to keep the low temperature. The gravimetric storage density of the liquid hydrogen in storage containers is about 25.9 wt.% (10.2 kWh/kg) and the volumetric energy density is about 2760kWh/m³ [15]. The improvements in insulation techniques and pressurization of the tank will have some effect on these figures. This type of storage has fast refueling (125 liter tank of liquid hydrogen can be refueled within only 3 minutes) [21].

2.2.2.3 – Metal hydrides storage

A special way of hydrogen storage is done by using metal hydride. Metal hydride is a metal or an alloy, which is able to bind the hydrogen chemically. This metal or alloy can store multiple hundreds of its capacity of hydrogen. When a hydride is formed with a metal or an alloy, heat is generated, i.e., the process is exothermic. Conversely, in order to release hydrogen from a metal hydride, heat must be supplied, i.e., the process is endothermic. These processes can be represented by the following chemical reactions [9]:

- Charging or absorption process : $M + xH_2 \rightarrow MH_{2x}$
- Discharging or desorption process: $MH_{2x} \rightarrow M + xH_2$

where M represents the hydriding substance, a metal or an alloy. The rate of these reactions increases with the surface area. Therefore, in general, the hydriding substances are used a powder to speed up

the reactions. MH is the metal hydride, X is ratio of the number of hydrogen atoms to the number of hydriding substance atoms. During the formation of the metal hydride hydrogen molecules are split and hydrogen atoms are inserted in spaces inside the lattice of the metals or alloys. In such a way an effective storage is created comparable to the density of liquid hydrogen. However, when the mass of the metal or alloy is taken into account then the metal hydride gravimetric storage density is comparable to storage of pressurized hydrogen. The best achievable gravimetric and volumetric hydrogen storage densities are about 0.07kg/kg of metal, and 101kg/m³ of metal respectively, for a high temperature hydride such as MgH₂. Also, the gravimetric and volumetric energy storage densities of this metal hydride are 2.8kWh/kg and 4000kWh/m³, respectively [18] and [22]. During the storage process (charging) heat is released which must be removed in order to achieve the continuity of the reaction. During the hydrogen release process (discharging) heat must be supplied to the storage tank.

Two ways can be used for storing electric energy in hydriding substances. In one of the methods, DC energy is used to electrolyse the water, and the hydrogen produced is stored in a hydriding substance. When electric energy is needed, the hydrogen is released from the hydriding substance by heating and used in a fuel cell to produce DC energy. Heat from fuel cell can be used to release hydrogen from the metal hydride. In the second method, one electrode of the electrolyser is covered with a hydriding substance [21]. During the electrolysis of water, the hydrogen produced on the electrode surface is immediately absorbed by the hydriding substance covering the electrode. Then, when electric energy is needed, the electrolyser operates in a reverse mode as a fuel cell using the hydrogen released from the metal hydride to produce electric energy.

Metal hydride process is expensive and sensitive against impurities and has finite lifetime. On the other hand, this kind of storage is relatively safe because the hydrogen is bound to a metal.

2.3 – Control Strategy

In Figure 2.3 the diagram of our control strategy for the system under study can be seen. The parameters showing in the figure are:

- P_s : This is the power by the solar cells
- P_l : This is the load
- P_{fcr} : This is the rated power of the fuel cell stack
- SOC: This is the state of charge of the battery
- P_{max} : This is the maximum pressure of the hydrogen tank
- P_{min} : This is the minimum pressure of the hydrogen tank
- P_{fc} : This is the power the fuel cell has to provide
- P_{el} : This is the power that the electrolyser will convert into hydrogen
- P_b : This is the power input/output of the battery
- E_s : This is the emergency signal. When it is 1 the system has to stop
- P_d : This is the power that is going to be dumped as excess power

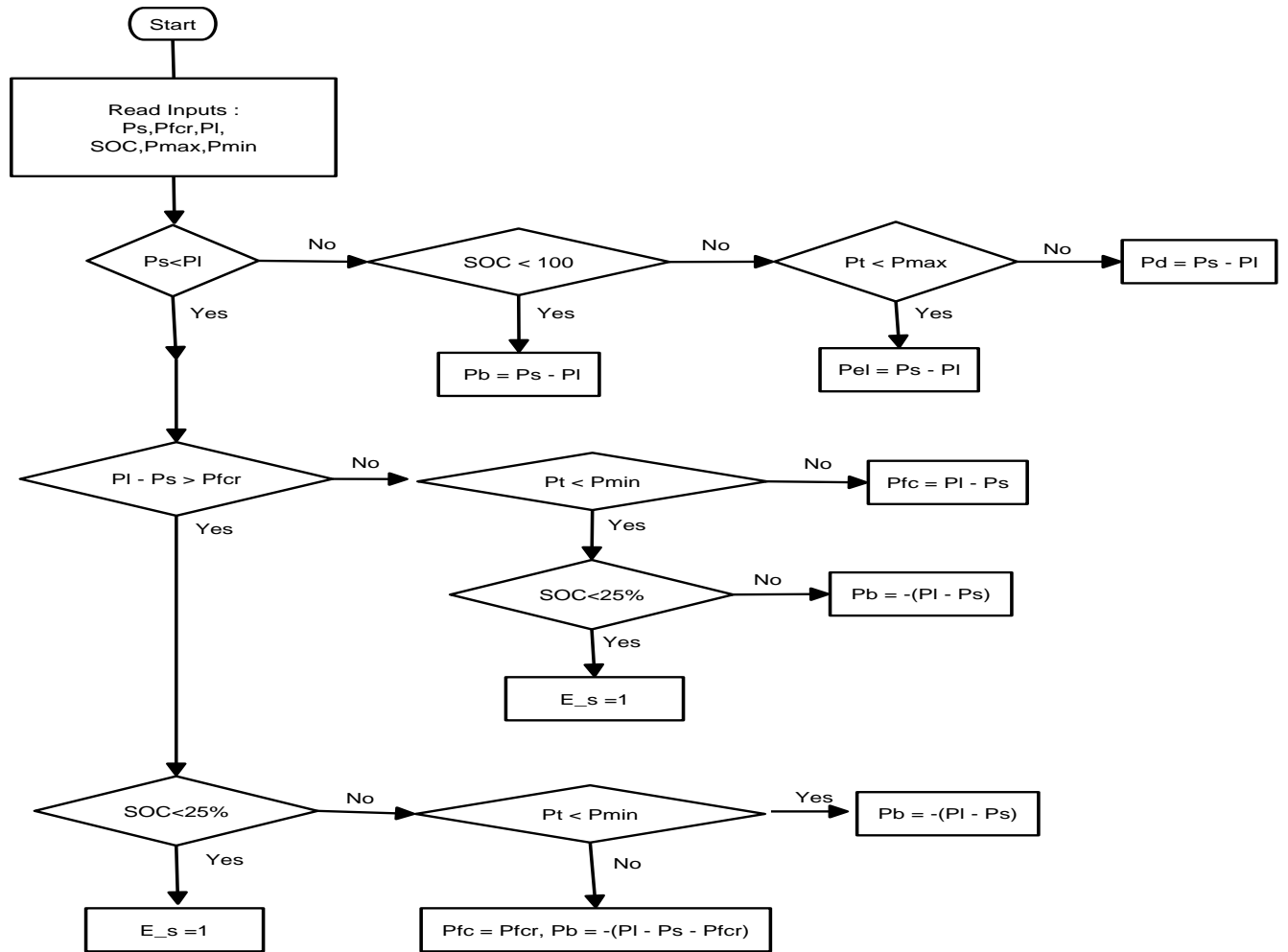


Figure 2.3: Control strategy diagram

In words, the control strategy works in the following way: If there is power surplus by the PV generator, then that power will either charge the battery until it is full, or, if the battery is already full, it will be converted by the electrolyser to hydrogen which will be stored in the tank. If the hydrogen tank is full, then the power surplus will be dumped as excess power. The storage tank had to be sized carefully so as to store as much power as possible during the summer, and waste as little as possible.

If there is power shortage, then the controller checks if that power can be provided by the fuel cell stack. If not, then the controller checks if the tank has enough pressure for the fuel cell stack to operate, and if it has, then the fuel cell stack provides its rated power and the rest if provided by the battery. If the battery is not charged enough then the emergency signal is set to 1 and the system must stop. If the power shortage is smaller than the rated power of the fuel cell stack, then, if there is enough pressure in the tank, the stack produces the necessary power. If there is not enough pressure, the controller tries to

take the necessary power from the battery, and if the battery is not charged enough, then the emergency signal is set to 1 and the system has to stop.

The fuel cell stack in the system studied has a rated power of 1KW, and the load has a maximum value of about 850KW, so the battery can only operate when the hydrogen tank is empty. Also the operating and stand-by power of each component was not taken into account due to lack of the necessary data.

2.4 – Conclusion

This chapter reviews most of the components in our system. The components not discussed in this chapter are the conditioning units and the battery, as, for their modeling, the blocks provided by Simulink were used. The following comments are worth to be mentioned about this system:

- 1 To increase the available energy efficiency of the PVFC hybrid system, the PV energy must be generated with highest efficiency before converting and storing it in the form of hydrogen.
- 2 The compressed hydrogen storage process is the best alternative relative to other storage processes where energy densities are not critical. The usefulness of compressed hydrogen might rise if its container is made from some composite materials, which enable increasing pressured hydrogen gravimetric energy density and thus decreasing the storage costs. Liquefied hydrogen suits for large size applications where the additional cost of the liquefaction facility does not matter. Metal hydrides might be the best for small size applications because of its high energy storage ability [22].
- 3 A short term energy storage, in this case the battery, is important to provide the balance of active and reactive power needed during the momentary load variation period. It also improves the power quality and efficiency of the systems. Also, it is used to reduce the capital expenses by allowing the systems to be sized more closely to the steady state power requirements, rather than over-sizing the generator to meet transient loading requirements. Therefore, the photovoltaic hydrogen fuel cell hybrid system with battery can serve dynamic loads and also provide power conditioning for grid connected or stand-alone system.

Chapter 3-PV Generator

3.1 PV Cell

The modeling of the characteristics of a PV cell is possible with the use equivalent electric circuits. In this paper two models will be discussed, the one-diode model and the two diode model.

3.1.1 One-diode model

The simplest model of a PV cell is shown as an equivalent circuit below that consists of an ideal current source in parallel with an ideal diode. The current source represents the current generated by photons (I_{ph}) and its output is constant under constant temperature and constant incident irradiation of light.

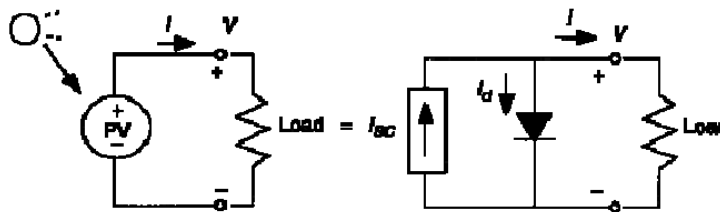


Figure 3.1: One-diode model

There are two key parameters frequently used to characterize a PV cell. Shorting together the terminals of the cell, as shown in figure 3.2(a), the photon generated current will follow out of the cell as a short circuit current (I_{sc}). Thus $I_{ph} = I_{sc}$. As shown in figure 3.2(b), when there is no connection to the PV cell (open-circuit), the photon generated current is shunted internally by the intrinsic p-n junction diode. This gives the open-circuit voltage (V_{oc}). The PV module or cell manufacturers usually provide the values of these parameters in their datasheets.

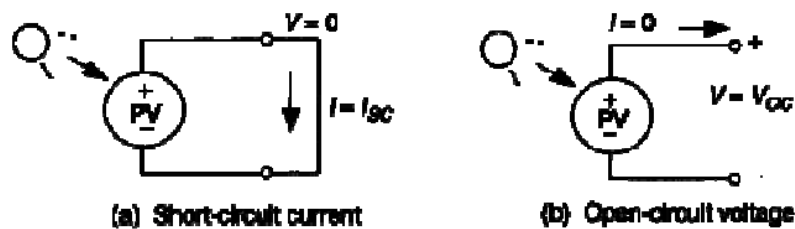


Figure 3.2: Short circuit and open circuit conditions

The output current (I) of the PV cell is found by applying the Kirchoff's current law (KCL) on the equivalent circuit shown in Figure 3.1 .

$$I = I_{sc} - I_d \quad (3-1)$$

Where: I_{sc} is the short circuit current that is equal to the photon generated current and I_d is the current shunted through the intrinsic diode.

The diode current (I_d) is given by the Shockley's diode equation :

$$I_d = I_0(e^{qV_d/KT} - 1) \quad (3-2)$$

Where: I_0 is the reverse saturation current of the diode (A),

q is the electron charge ($1.602 \times 10^{-19} \text{ C}$),

V is the voltage across the diode (V)

k is the Boltzmann's constant ($1.381 \times 10^{-23} \text{ J / K}$)

T is the junction temperature (K)

Replacing I_d of the equation 3-1 by the equation 3-2 gives the current voltage relationship of the PV cell:

$$I = I_{sc} - I_0(e^{qV/KT} - 1) \quad (3-3)$$

Where: V is the voltage across the PV cell and I is the output current from the cell

The reverse saturation current of diode (I_0) is constant under the constant temperature and found by setting the open-circuit condition as shown in Figure 3.2(b). Using the equation (3-3), let $I = 0$ (no output current) and solve for I_0 :

$$0 = I_{sc} - I_0(e^{qV_{oc}/KT} - 1) \quad (3-4)$$

$$I_{sc} = I_0(e^{qV_{oc}/KT} - 1) \quad (3-5)$$

$$I_0 = \frac{I_{sc}}{e^{qV_{oc}/KT} - 1} \quad (3-6)$$

To a very good approximation, the photon generated current, which is equal to I_{sc} , is directly proportional to irradiance, the intensity of illumination, to PV cell[23]. Thus, if the value I_{sc} is known from the datasheet, under the standard test conditions, $G_0 = 1000 \text{ W / m}^2$ at the air mass (A.M.)=1.5, then the photon generated current at any other irradiance $G(\text{W / m}^2)$ is given by:

$$I_{sc_G} = \left(\frac{G}{G_0}\right) I_{sc_G_0} \quad (3-7)$$

3.1.2 The two-diode model

There are a few things that have not been taken into account in the previous model and can affect the efficiency of a PV cell in practice. A brief description of these factors is given here:

3.1.2.1 Series Resistance

In a practical PV cell there is a series of resistance in a current path through the semiconductor material, the metal grid, contacts and current collecting bus [24]. These resistive losses are lumped together as a series resistor (R_s). This resistance has a very substantial effect in a PV module that consists of many series-connected cells, as its value is multiplied by the number of cells.

3.1.2.2 Parallel Resistance

This is also called shunt resistance. It is a loss associated with a small leakage of current through a resistive path in parallel with the intrinsic device [24]. This can be represented by a parallel resistor (R_p). Its effect is as important as R_s and it will only become noticeable in the case of parallel connected PV modules.

3.1.2.3 Recombination

Recombination in the depletion region of PV cells provides non-Ohmic current paths in parallel with the intrinsic PV cell [24]. As shown in Figure 3.3, this can be represented by the second diode (D_2) in the equivalent circuit:

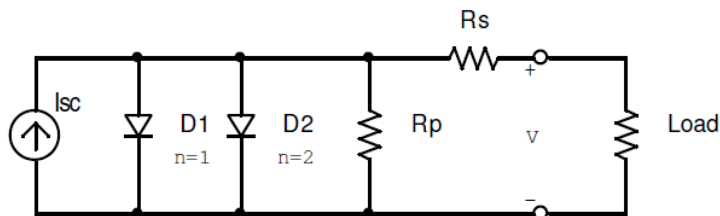


Figure 3.3: Two-diode model

Summarizing these effects, the current-voltage relationship of a PV cell is written as:

$$I = I_{sc} - I_{01} \left[e^{\frac{q(V+IR_s)}{KT}} - 1 \right] - I_{02} \left[e^{\frac{q(V+IR_s)}{2KT}} - 1 \right] - \left(\frac{V + IR_s}{R_p} \right) \quad (3-8)$$

It is possible to combine the first diode (D_1) and the second diode (D_2) and rewrite the equation (3-8) in the following form:

$$I = I_{sc} - I_0 \left[e^{\frac{q(V+IR_s)}{nKT}} - 1 \right] - \left(\frac{V+IR_s}{R_p} \right) \quad (3-9)$$

Where: n is known as the “ideality factor” and takes values between one and two [7].

3.2 PV Module

A single PV cell produces an output of less than 1V (about 0.6 for crystalline-silicon cells), thus a number of a number of PV cells is connected in series to provide a desired output voltage. So when series-connected PV cells are put in a frame, the result is a PV module. Most commercially available PV modules with crystalline-Si cells have either 36 or 72 series-connected cells. When PV cells are connected together in series the output current is the same as in one cell but the voltage output is the sum of each cell voltage. Also modules can be connected together in series or in parallel to provide the necessary current or voltage. In that case the connect PV modules form a PV array.

For the modeling of the PV module the design strategy is the same as it was for the PV cell. The parameters are all the same, but only a voltage parameter (such as open-circuit voltage) is different and must be divided by the number of cells.

The study done by Walker [25] of University of Queensland, Australia uses the electric model with moderate complexity shown in figure (3.4) and provides fairly accurate results. The model consists of a current source (I_{sc}), a diode (D) and a series resistance (R_s). Parallel resistance R_p can be neglected as its effect is not important in a single module. Temperature effects on the short circuit current (I_{sc}) and the reverse saturation current of the diode (I_0) are also included to increase the accuracy of the model. It uses a single diode with the diode ideality factor (n) set to achieve the best $I-V$ curve match.

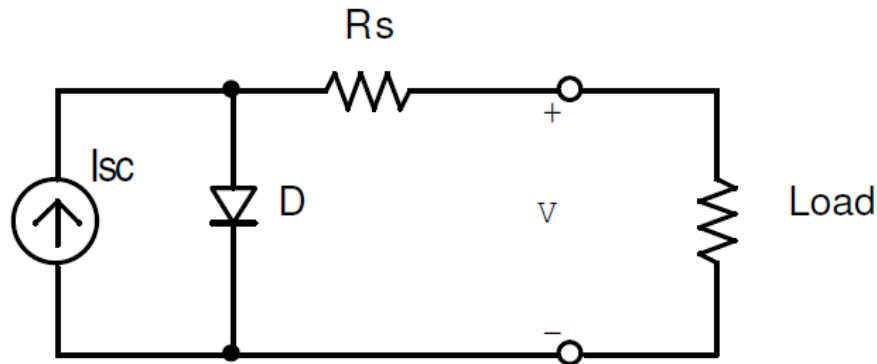


Figure (3.4) : Equivalent circuit used

So, assuming that $R_p = \infty$ in order to take out the effect of the parallel resistance, equation (3-9) becomes:

$$I = I_{sc} - I_0 \left[e^{\frac{q(VIR_s)}{nkT}} - 1 \right] \quad (3-10)$$

where: I is the module current (A)

V is the cell voltage (V)

T is the cell temperature (K)

The short-circuit current (I_{sc}) is calculated first at a given cell temperature (T):

$$I_{sc_T} = I_{sc_Tref} [1 + a(T - T_{ref})] \quad (3-11)$$

where: I_{sc} at T_{ref} is given in the datasheet (A)

T_{ref} is the reference temperature of the PV cell (298 K in this case)

a is the temperature coefficient of I_{sc} in percent change per degree temperature (datasheet)

The short-circuit current (I_{sc}) is proportional to the intensity of irradiance, thus I_{sc} at given irradiance (G) is:

$$I_{sc_G} = \left(\frac{G}{G_0} \right) I_{sc_G0} \quad (3-12)$$

where: $G_0 = 1000W / m^2$, the nominal value for the intensity of irradiance

The reverse saturation current of diode (I_0) at the reference temperature (T_{ref}) is given by equation (3-6) with the diode ideality factor added:

$$I_0 = \frac{I_{sc}}{(e^{(qV_{oc}/nkT)} - 1)} \quad (3-13)$$

The reverse saturation current (I_0) is temperature dependant and the I_0 at a given temperature (T) is calculated by the following equation [25]:

$$I_{0_T} = I_{0_Tref} \left(\frac{T}{T_{ref}} \right)^{3/n} * e^{\frac{-qE_g}{nk} (1/T - 1/T_{ref})} \quad (3-14)$$

The diode ideality factor (n) is a constant that takes values between one and two (one is for the value for the ideal diode). The best way to estimate it accurately is by curve-fitting [25].

The series resistance (R_s) of the PV cell has a large impact on the slope of the $I - V$ curve near the open-circuit voltage (V_{oc}), hence the value of R_s is calculated by evaluating the slope $\frac{dV}{dI}$ of the $I - V$ curve at the V_{oc} [25]. The equation for R_s is derived by differentiating the equation (3-10) and then rearranging it in terms of R_s .

$$I = I_{sc} - I_0 \left[e^{q \left(\frac{V + IR_s}{nkT} \right)} - 1 \right] \quad (3-15)$$

$$dI = 0 - I_0 q \left(\frac{dV + R_s dI}{nkT} \right) e^{q \left(\frac{V + IR_s}{nkT} \right)} \quad (3-16)$$

$$R_s = - \frac{dI}{dV} - \frac{nkT / q}{I_0 e^{q \left(\frac{V + IR_s}{nkT} \right)}} \quad (3-17)$$

Then evaluate the equation (3-17) at the open-circuit voltage that is $V = V_{oc}$ (also let $I = 0$).

$$R_s = - \frac{dV}{dI} \Big|_{V_{oc}} - \frac{nkT/q}{I_o \cdot e^{\frac{qV_{oc}}{nkT}}}$$

where: $\frac{dV}{dI}$ at V_{oc} is the slope of the $I - V$ curve at V_{oc} (use the I-V curve in the datasheet and then divide it by the number of cells in series

V_{oc} is the open-circuit voltage of the cell

The calculation using the slope of the $I - V$ curve published on the Sanyo Hip-215NKHE5 series datasheet gives a value of series resistance $R_s = 5.2m\Omega$.

Finally, it is possible to solve the equation (3-10). It is, however, complex because the solution of current is recursive by inclusion of a series resistance in the model. Although it may be possible to find the answers by simple iterations, the Newton's method is chosen for rapid convergence of the answer [25]. The Newton's method is described as:

$$x_{n+1} = x_n - \frac{f(x_n)}{f'(x_n)} \quad (3-19)$$

where: $f'(x)$ is the derivative of the function, $f(x) = 0$, x_n is a present value, and x_{n+1} is a next value.

Rewriting the equation (3-10) gives the following function:

$$f(I) = I_{sc} - I - I_0 \left[e^{q \left(\frac{V + IR_s}{nkT} \right)} - 1 \right] \quad (3-20)$$

Plugging this into the equation (3-19) gives a following recursive equation, and the output current (I) is computed iteratively.

$$I_{n+1} = I_n - \frac{I_{sc} - I_n - I_0 \left[e^{q \left(\frac{V + I_n R_s}{nkT} \right)} - 1 \right]}{-1 - I_0 \left(\frac{qR_s}{nkT} \right) e^{q \left(\frac{V + I_n R_s}{nkT} \right)}} \quad (3.21)$$

For the implementation of this formula in the Simulink modeling of the system an embedded Matlab code is used. This Matlab code performs the calculation 5 times iteratively to ensure convergence of the results. More detailed information about this can be found in Chapter 4 where the Simulink implementation of the mathematical model is discussed.

3.3 – Simulink implementation of PV Generator

3.3.1 - PV Generator model

Sanyo HIP-215NKHE5 was chosen for implementation in Simulink. The formulas discussed in Chapter 3 were used and the constants were taken from the manufacturer's datasheet. The specifications of this PV module can be seen on Table (3.1) below:

Models HIP-xxxNKHE5		
Electrical data	215	214
Maximum power (Pmax) [W]	215	214
Max. power voltage (Vpm) [V]	42.0	41.9
Max. power current (Ipm) [A]	5.13	5.12
Open circuit voltage (Voc) [V]	51.6	51.5
Short circuit current (Isc) [A]	5.61	5.60
Warranted min. power (Pmin) [W]	204.3	203.3
Maximum over current rating [A]	15	
Output power tolerance [%]	+10 / -5	
Max. system voltage [Vdc]	1000	
Temperature coeff. of Pmax [%/°C]	-0.30	
Temperature coeff. of Voc [V/°C]	-0.129	-0.129
Temperature coeff. of Isc [mA/°C]	1.68	1.68
NOCT [°C]	48.0	
Note 1: Standard test conditions: Air mass 1.5, Irradiance = 1000 W/m ² , Cell temperature = 25 °C.		
Note 2: The values in the above table are nominal.		

Table 3.1: Datasheet for the PV module

The interface of our PV generator with the rest of the system can be seen below in Figure (3.5)

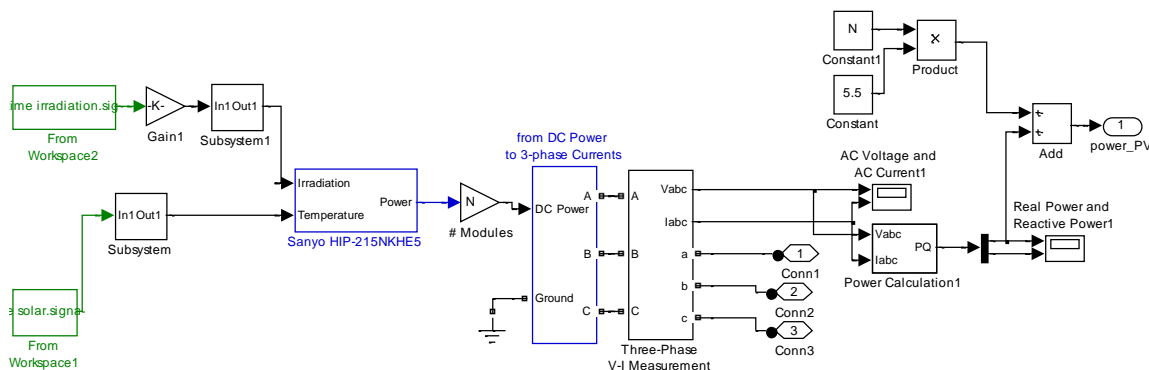


Figure 3.5: PV subsystem

This block is called “Solar Subsystem” and uses the “From Workspace” blocks of Simulink to get the necessary data for temperature and irradiation. Then these data enter the “Sanyo HIP-215NKHE5” block whose output is the DC power provided by the PV module. After this block the power is multiplied by N, where N is the number of PV modules of our system. Then the DC power is converted to AC power and is added to the virtual grid used as a voltage regulator. The results of a simulation of the Solar Subsystem for the first week of January can be seen in the scope below:

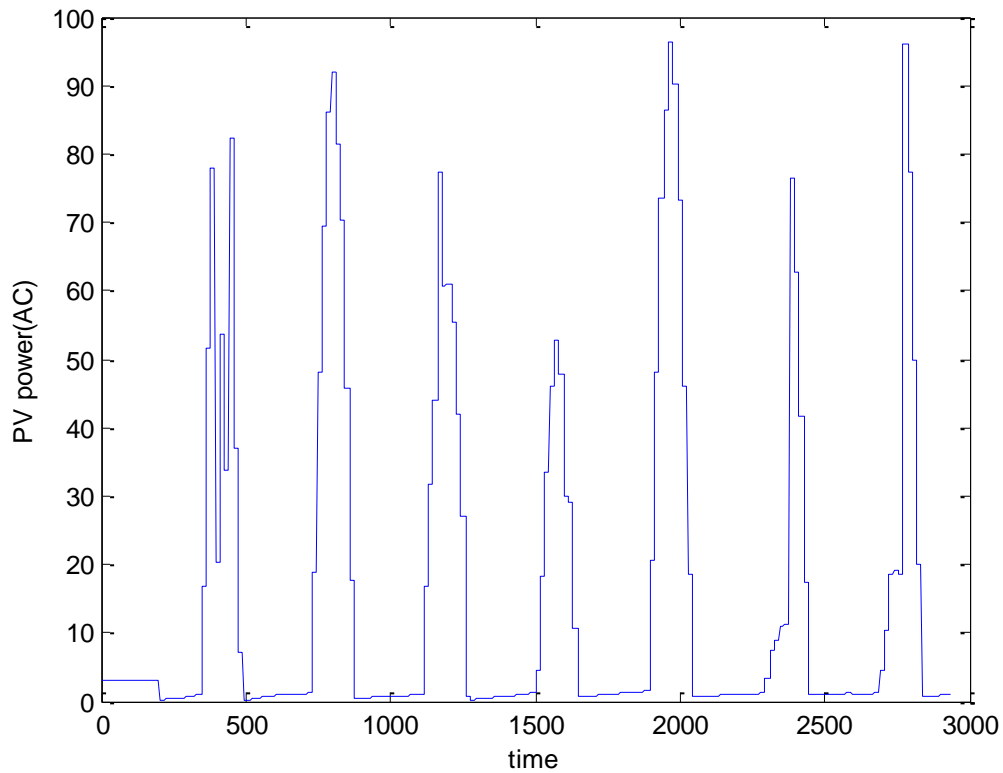


Figure 3.6: PV power for one PV module on first week of winter

The PV module provides less power than the one specified in the datasheet but this normal because the irradiation at the first week of January is considerably less than $1000W / m^2$.

The model was also tested for different voltages and temperatures and the resulting diagram can be seen in Figure (3.7) below:

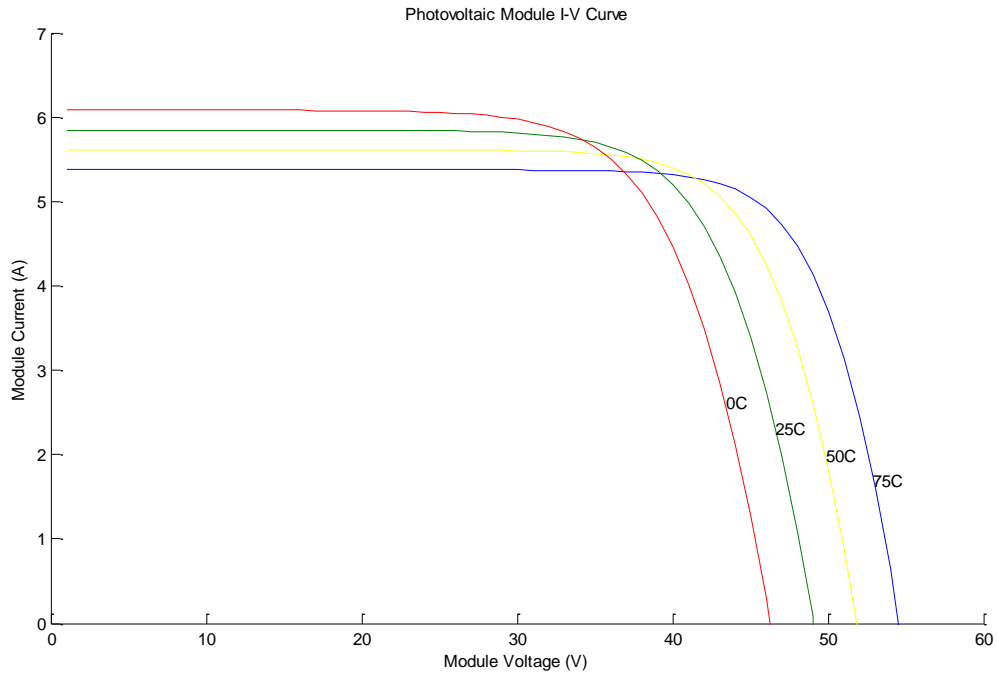


Figure 3.7: Operation of a PV module with varied temperature

The results of the simulation of the “PV_cell” model correspond well to the physical properties of a photovoltaic module. For a temperature of $25^{\circ}C$ and a given irradiance of $1000W/m^2$ it was expected to provide a voltage of 51.6 V according to the datasheet, while it provides a voltage of 49V. That means that the model is close to the real performance of Sanyo HIP-NKHE5 module.

3.3.2 - PV cell model

The model for a single PV cell is shown in the figure (3.8) below:

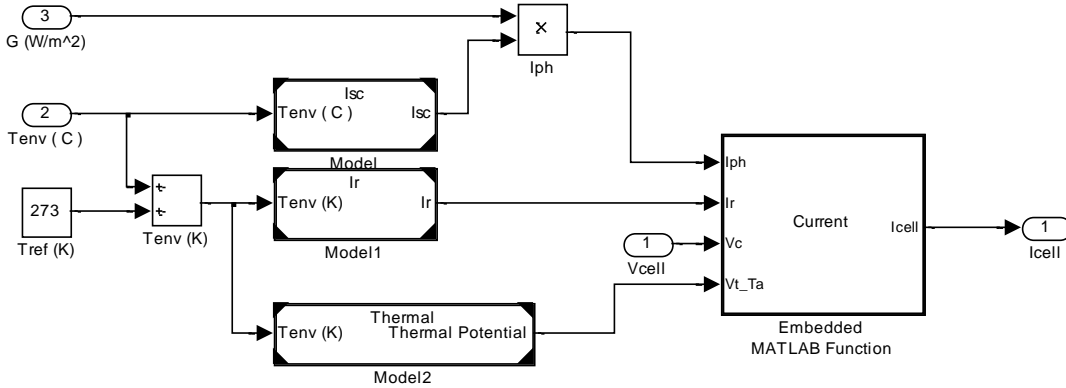


Figure 3.8: Simulink model for a single PV cell

This model takes as inputs the irradiation and the temperature and calculates the correspondent short-circuit current (I_{sc}), reverse saturation current (I_r), photon current (I_{ph}) and thermal potential (V_{t_Ta}). The blocks calculating the parameters mentioned above will be discussed later on this chapter. The output of this block, I_{cell} , is calculated using an embedded Matlab function which implements, as mentioned in Chapter 3, this formula:

$$I_{n+1} = I_n - \frac{I_{sc} - I_n - I_0 \left[e^{\frac{q(V+I_nR_s)}{nkT}} - 1 \right]}{-1 - I_0 \left(\frac{qR_s}{nkT} \right) e^{\frac{q(V+I_nR_s)}{nkT}}}$$

The reason the Matlab function was used and not a Simulink block is that the formula contains a loop which, if implemented using Simulink components, adds unnecessary complexity and delay to the whole system. The Matlab code can be found in Appendix.

The Simulink model for the calculation of short-circuit current (I_{sc}) can be seen in Figure (3.9) below:

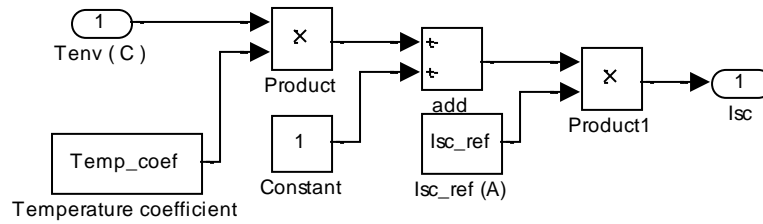


Figure 3.9: Simulink model for calculation of short-circuit current

This model is the implementation in Simulink of the formula:

$$I_{sc_T} = I_{sc_Tref} [1 + a(T - T_{ref})]$$

I_{sc_ref} and a can be found in the datasheet. I_{sc_T} is the short-circuit current for temperature T .

The Simulink model for the calculation of reverse saturation (I_r) current can be seen in Figure (3.10) below:

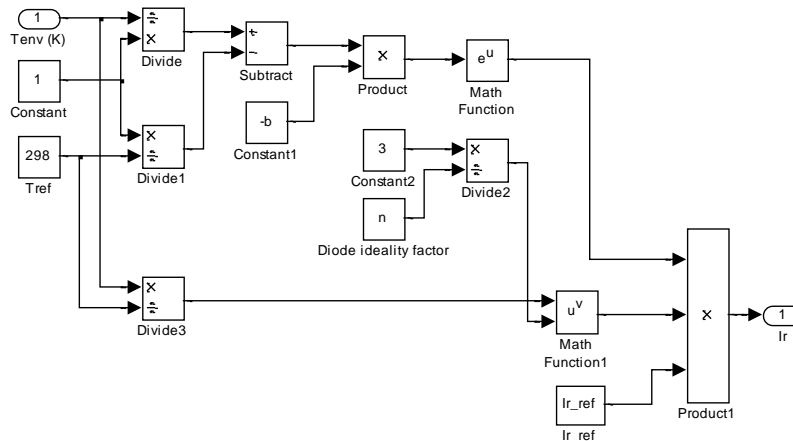


Figure 3.10: Simulink model for calculation of reverse saturation current

This model is the implementation in Simulink of the formula:

$$I_{0_T} = I_{0_Tref} \left(\frac{T}{T_{ref}} \right)^{3/n} * e^{\frac{-qE_g}{nk} (1/T - 1/T_{ref})}$$

I_{0_Tref} is the reverse saturation current for the reference temperature and can be calculated by the formula:

$$I_{0_Tref} = \frac{I_{sc}}{(e^{(qV_{oc}/nkT)} - 1)}$$

The Simulink model for the calculation of the thermal potential can be seen in Figure (3.11) below:

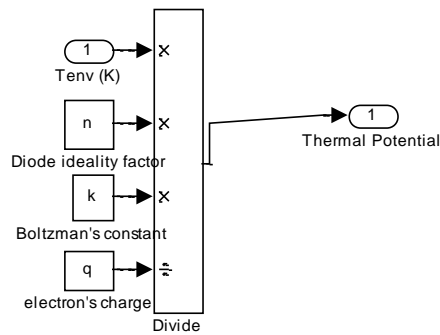


Figure 3.11: Simulink model for calculation of thermal potential

This model is the implementation in Simulink of the formula:

$$V_t = nkT / q$$

where: n is the diode ideality factor (1.62)

k is Boltzmann's constant ($1.381 * 10^{-23}$)

T is temperature of the photovoltaic cell

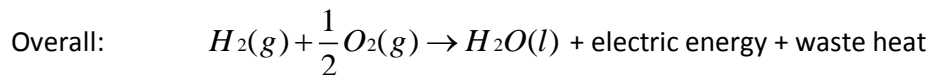
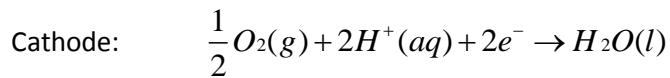
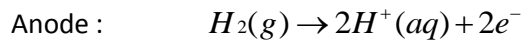
q is the electron's charge ($1.602 * 10^{-19}$ eV)

Chapter 4 – Fuel cell

4.1 – Introduction

A fuel cell consists of a negatively charged electrode (anode), a positively charged electrode (cathode) and an electrolyte membrane. Hydrogen is oxidized at the anode and oxygen is reduced at the cathode. Protons are transported from the anode to the cathode through the electrolyte membrane, and the electrons are carried to the cathode over the external circuit. In nature, molecules cannot stay in an ionic state, therefore they immediately recombine with other molecules in order to return to the neutral state. Hydrogen protons in fuel cells stay in the ionic state by travelling from molecule to molecule through the use of special materials. The protons travel through a polymer membrane made of persulfonic acid groups with a Teflon backbone. The electrons are attracted to conductive materials and travel to the load when needed. On the cathode, oxygen reacts with protons and electrons, forming water and producing heat. Both the anode and cathode contain a catalyst to speed up the electrochemical processes, as shown in figure 4.1.

A typical PEM fuel cell (proton exchange membrane fuel cell) has the following reactions:



Reactants are transported by diffusion and/or convection to the catalyzed electrode surfaces where the electrochemical reactions take place. The water and waste heat generated by the fuel cell must be continuously removed and may present critical issues for PEM fuel cells.

The basic PEM fuel cell stack consists of a proton exchange membrane (PEM), catalyst and gas diffusion layers, flow field plates, gaskets and endplates as shown in Table 4.1: The actual fuel cell layers are the PEM, gas diffusion and catalyst layers. These layers are “sandwiched” together using various processes, and are called the membrane electrode assembly (MEA). A stack with many cells has MEAs “sandwiched” between bipolar flow field plates and only one set of endplates.

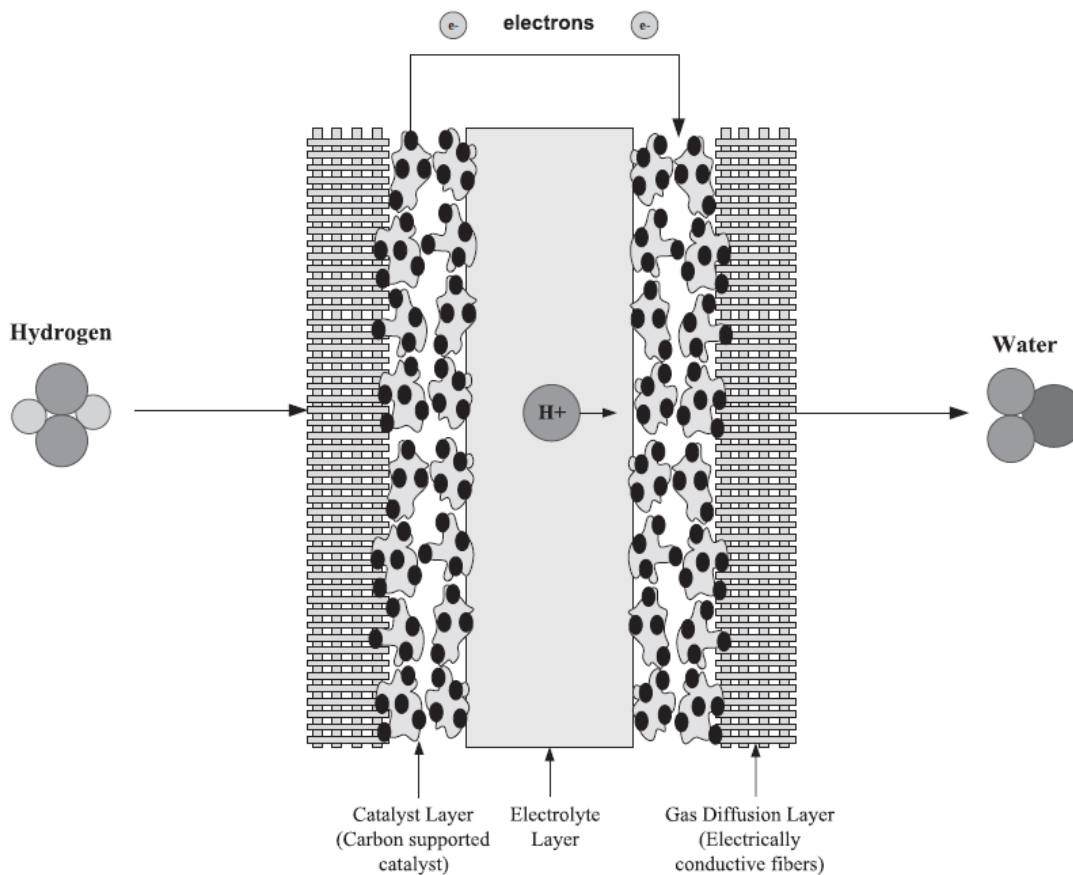


Figure 4.1: A single PEM fuel cell configuration.

Some advantages of the fuel cell systems are as follows:

- Fuel cells have the potential for a high operating efficiency
- There are many types of fuel sources, and methods of supplying fuel to a fuel cell
- Fuel cells have a highly scalable design
- Fuel cells produce no pollutants
- Fuel cells are low maintenance because they have no moving parts
- Fuel cells do not need to be recharged, and they provide power instantly when supplied with fuel.

Some limitations common to all fuel cell systems are as follows:

- Fuel cells are currently costly due to the need for materials with specific properties. There is an issue with finding low-cost replacements. This includes the need for platinum and Nafion material.
- Fuel reformation technology can be costly and heavy and needs power in order to run.
- If another fuel besides hydrogen is fed into the fuel cell, the performance gradually decreases over time due to catalyst degradation and electrolyte poisoning.

<i>Component</i>	<i>Description</i>	<i>Common Types</i>
Proton exchange membrane	Enables hydrogen protons to travel from the anode to the cathode.	Persulfonic acid membrane (Nafion 112, 115, 117)
Catalyst layers	Breaks the fuel into protons and electrons. The protons combine with the oxidant to form water at the fuel cell cathode. The electrons travel to the load.	Platinum/carbon catalyst
Gas diffusion layers	Allows fuel/oxidant to travel through the porous layer, while collecting electrons	Carbon cloth or Toray paper
Flow field plates	Distributes the fuel and oxidant to the gas diffusion layer	Graphite, stainless steel
Gaskets	Prevent fuel leakage, and helps to distribute pressure evenly	Silicon, Teflon
End plates	Holds stack layers in place	Stainless steel, graphite, polyethylene, PVC

Table 4.1: Basic fuel cell components

4.2 – Fuel cell types

Leaving aside practical issues such as manufacturing and material costs, the two fundamental technical problems with fuel cells are the slow reaction rate, leading to low currents and power, and the fact that hydrogen is not a readily available fuel. To solve these problems many different fuel cell types have been tried. The different fuel cell types are usually distinguished by the electrolyte that is used, though there are always other important differences as well. The situation now is that six classes of fuel cells have emerged as viable systems for the present and near future. Basic information about these systems is given in Table 4.2.

The six types of fuel cell are:

1. PEM - Proton Exchange Membrane Fuel Cell
2. DMFC – Direct Methanol Fuel cell
3. AFC – Alkaline Fuel Cell
4. PAFC – Phosphoric Acid Fuel Cell
5. MCFC – Molten Carbonate Fuel Cell
6. SOFC – Solid Oxide Fuel Cell

In addition to facing different problems, the various fuel types also try to play to the strength of fuel cells in different ways.

Fuel cell type	Mobile ion	Operating temperature	Applications and notes
Alkaline (AFC)	OH^-	50–200°C	Used in space vehicles, e.g. Apollo, Shuttle.
Proton exchange membrane (PEMFC)	H^+	30–100°C	Vehicles and mobile applications, and for lower power CHP systems
Direct methanol (DMFC)	H^+	20–90°C	Suitable for portable electronic systems of low power, running for long times
Phosphoric acid (PAFC)	H^+	~220°C	Large numbers of 200-kW CHP systems in use.
Molten carbonate (MCFC)	CO_3^{2-}	~650°C	Suitable for medium- to large-scale CHP systems, up to MW capacity
Solid oxide (SOFC)	O^{2-}	500–1000°C	Suitable for all sizes of CHP systems, 2 kW to multi-MW.

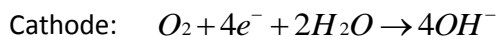
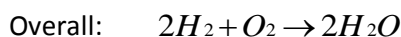
Table 4.2: Data for different types of fuel cells

Below the different types of fuel cells will be examined in the terms of their advantages and disadvantages. PEMFC will be discussed in greater detail later, as it is the one used in this system.

4.2.1 – AFC

In an alkaline electrolyte fuel cell hydroxyl (OH^-) ions are available and mobile. At the anode, these react with hydrogen, releasing energy and electrons, and producing water. At the cathode, oxygen reacts with electrons taken from the electrode, and water in the electrolyte, forming new OH^- ions.

The reactions taking place in an alkaline fuel cell are:



The advantages and limitations of AFC are listed below:

- + Low manufacturing and operation costs
- + Does not need heavy compressor
- + Fast cathode kinetics
- **Large size**

- Needs pure hydrogen and oxygen
- Use of corrosive liquid electrolyte

4.2.2 – PAFC

Phosphoric acid fuel cells (PAFC) are a type of fuel cell that uses liquid phosphoric acid as an electrolyte. PAFCs are appreciated by the industry and are suitable to use with a CHP as hybrid energy generator.

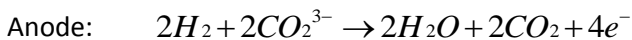
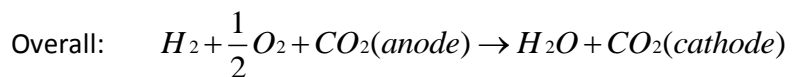
The advantages and limitations of PAFC are listed below:

- + Commercially available
- + Lenient to fuels
- + Produces heat for cogeneration
- Low efficiency
- Limited service life
- Expensive catalyst

4.2.3 – MCFC

Molten carbonate fuel cells (MCFCs) are high temperature fuel cells, operating at temperatures of 600° C and above. They are currently being developed for natural gas and coal-based power plants for electrical utility, industrial and military applications. MCFCs use an electrolyte composed of a molten carbonate salt mixture suspended in a porous, chemically inert ceramic matrix of beta-alumina solid electrolyte (BASE). Since they operate at extremely high temperatures non-precious metals can be used as catalysts at the anode and the cathode, reducing costs. [wikipedia]

The reactions taking place in a MCFC are:



The advantages and limitations of MCFC are listed below:

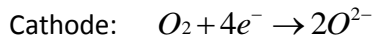
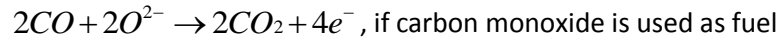
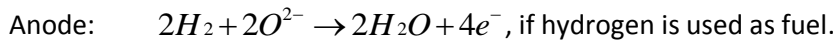
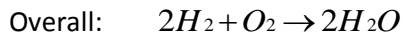
- + Highly efficient

- + Produces heat for cogeneration
- Electrolyte instability
- Limited service life

4.2.4 – SOFC

The SOFC is a complete solid-state device that uses an oxide ion-conducting ceramic material as the electrolyte. It is therefore simpler in concept than all the other fuel cell systems. Currently it is the least developed type of fuel cell but breakthroughs in cell material and stack design set off new research.

The reactions taking place in a SOFC are:



The advantages and limitations of SOFC are:

- + High efficiency
- + Lenient to fuels
- + Takes natural gas directly
- + No reformer
- + Produces heat for cogeneration
- High operating temp
- Exotic metals
- High manufacturing cost
- Oxidation issues
- Low specific power

4.3 – PEMFC

The proton exchange membrane fuel cell (PEMFC), also called the solid polymer fuel cell (SPFC), was first developed by General Electric in the United States in the 1960s for use by NASA on their first manned space vehicles. Its electrolyte is an ion conducting polymer, which is bonded with a catalyst porous electrode on each side. The basic principles of PEMFC operation were discussed at the introduction of this chapter, as well as the overall reaction and the reactions at the anode and the cathode.

The advantages and limitations of PEMFC are:

- + Most advanced in technological development and commercially available
- + Excellent for hydrogen operation
- + Rapid start-up and excellent dynamics
- + Simple system-layout and control
- + Compact design
- + Long operating life
- High manufacturing costs
- Needs pure hydrogen
- Heavy auxiliary equipment and complex heat and water management

In figure 4.2 a single PEMFC assembly can be seen. It is obvious that the designer of a fuel cell must take into account many factors such as the fuel and coolant flow, the avoidance of hydrogen leakage to the environment, or the most efficient electrolyte-catalyst-electrode contact.

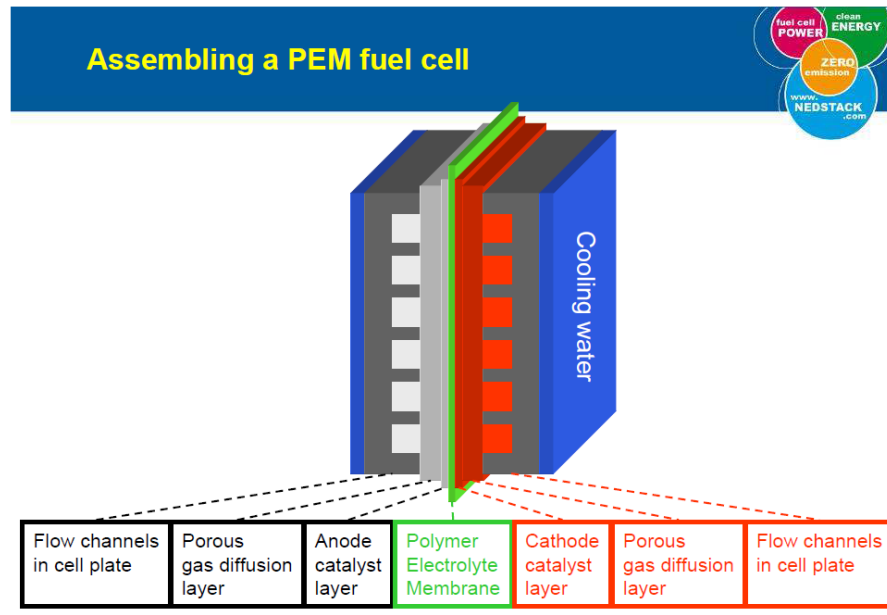


Figure 4.2: PEMFC assembly

4.3.1 – Polymer Electrolyte Membrane

The main function of the PEM is to allow the H^+ ions to pass through it, from the cathode to the anode. Also it has to provide electrical insulation so that the electrons cannot pass through it, as this would mean significant power loss for the fuel cell. Details for this will be discussed later, at the part of the chapter concerning voltage losses.

The most well-known and established material for the membrane is Nafion, which is a copolymer of Teflon-like backbone and perfluorosulfonic acid side chain. From the point of view of fuel cell use the main features of Nafion are that:

- It is chemically highly resistant
- It is strong (mechanically), and so can be made into very thin films, down to 50 μm
- It is acidic
- It can absorb large quantities of water
- If well-hydrated the H^+ ions can move freely through the material-it is good proton conductor

4.3.2 – Catalyst

The best catalyst for both the anode and the cathode is platinum. Its function is to facilitate the reactions taking place into the electrodes. The platinum catalyst is formed into very small particles on the surface of somewhat larger particles of finely divided carbon powders. The result in an idealized

form is shown in figure 4.3. The platinum is highly divided and spread out, so that a very high proportion of the surface area will be in contact with the reactants.

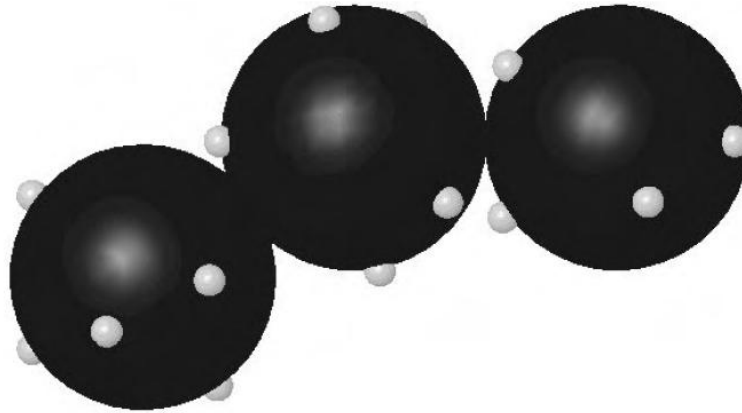


Figure 4.3: The structure of carbon-supported catalyst

4.3.3 – Gas-diffusion layer

It is either carbon paper or carbon cloth material. Its functions can be seen below:

- Transport the electrons to and from the catalyst
- Transport reactant gases to the catalyst
- Transport product water away from cathode catalyst
- Provide mechanical strength to the membrane-electrode assembly

4.3.4 – Water Management

A very important subject for the PEMFCs is the water management. There must be sufficient water content in the polymer electrolyte as the proton conductivity is directly proportional to it. However, there must not be so much water that the electrodes that are bonded to the electrolyte flood, blocking the pores in the electrodes or the gas-diffusion layer. A balance therefore is needed.

During the operation of the fuel cell, while the H^+ ions pass through the electrolyte, they drag with them between one and five water molecules, a phenomenon which is called electro-osmotic drag. This means that, especially at high current densities, the anode side of the electrolyte can become dried-out, even if the cathode is well-hydrated. Another major problem is the drying effect of air at high temperatures. One common way to solve these problems is to humidify the air, the hydrogen, or both before they enter the fuel cell, which greatly improves the fuel cell performance.

4.4 – Mathematical Modeling of PEMFC

The PEM fuel cell model here depends on the physical and theoretical analysis, so-called analytical model. At first the ideal performance of the unit is determined, and then the different types of losses are calculated and deducted from it, to end up with a good estimation of the actual operation. To simplify the analysis of the model, water management analysis has to be excluded.

4.4.1 – Energy and EMF of the PEMFC

With the basic operation of a fuel cell already explained, the inputs and the outputs of the unit are shown in Figure (4.4).

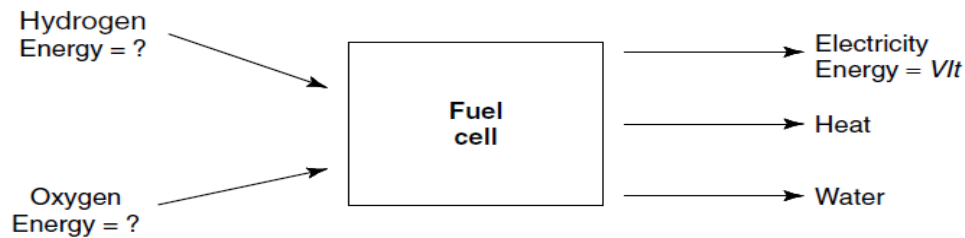


Figure 4.4: Fuel cell inputs and outputs

The electrical power and energy output can be calculated by the formulas:

Electrical Power: $Power = VI$ (4-1)

Electrical Energy: $Energy = VIt$ (4-2)

The energy of the chemical input and output is not so easily defined. The energy that is important in the case of fuel cells is the "Gibbs free energy". This can be defined as the "energy available to do external work, neglecting any work done by changes in pressure and/or volume". In a fuel cell, the "external work" involves moving electrons round an external circuit, since any work done by a change in volume between the input and the output is not harnessed by the fuel cell. So in order to find the energy released in the unit, the difference in the "Gibbs free energy" of the reactants and the products must be determined. That is given by the formula:

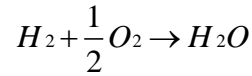
$$\Delta G = G \text{ of products} - G \text{ of reactants} \quad (4-3)$$

Or, if the reactants and products are in the standard conditions ($T_0 = 298.15K$, $p_0 = 100kPa$), then equation 4-3 becomes:

$$\Delta G_f = G_f \text{ of products} - G_f \text{ of reactants} \quad (4-4)$$

where: G_f is called "Gibbs free energy of formation".

The "Gibbs free energy of formation" is not constant. It changes with temperature and state (liquid or gas). Table 4.3 below shows ΔG_f for the basic hydrogen fuel cell operation:



Form of water product	Temperature (°C)	$\Delta \bar{g}_f$ (kJ mol ⁻¹)
Liquid	25	-237.2
Liquid	80	-228.2
Gas	80	-226.1
Gas	100	-225.2
Gas	200	-220.4
Gas	400	-210.3
Gas	600	-199.6
Gas	800	-188.6
Gas	1000	-177.4

Table 4.3: ΔG_f for the basic reaction in a hydrogen fuel cell

If there are no losses in a fuel cell, then all Gibbs free energy is converted into electrical energy. By that the operating cell voltage (OCV) of a fuel cell can be found.

According to the basic hydrogen fuel cell operation, two electrons pass round the external circuit for each water molecule produced and each molecule of hydrogen used. So, for one mole of hydrogen used, $2N$ electrons pass through the external circuit, where N is Avogadro's number. If $-e$ is the charge on one electron, then the charge that flows is:

$$-2Ne = -2F \text{ (Coulombs)} \quad (4-5)$$

where: F is the Faraday constant or the charge on one mole of electrons.

If E is the voltage of the fuel cell, then the electrical work done by moving this charge around the circuit is:

$$\text{Electrical work done} = \text{Charge} \times \text{Voltage} = -2FE \text{ joules}$$

If the system is reversible (or has no losses), then this electrical work done will be equal to the Gibbs free energy released ΔG_f . So:

$$\Delta G_f = -2FE \quad (4-6)$$

Thus:

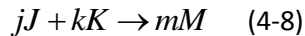
$$E = -\frac{\Delta G_f}{2F} \quad (4-7)$$

Equation 4-7 gives the electromotive force (EMF) or reversible open circuit voltage of the hydrogen fuel cell.

4.4.2 – Nernst equation

In the previous section, it was noted that the Gibbs free energy changes in a chemical reaction vary with temperature. Equally important, though more complex, are the changes in Gibbs free energy with reactant pressure and concentration.

Consider a general reaction such as:



where j moles of J react with k moles of K to produce m moles of M . Each of the reactants and the products has an associated “activity”. This activity is designated by a , a_j and a_k being the activity of the reactants and a_m the activity of the product. In the case of ideal gases it can be shown that :

$$a = \frac{P}{P_0} \quad (4-9)$$

where P is the pressure or partial pressure of the gas and P_0 is standard pressure, $0.1MPa$.

The activities of the reactants and products modify the Gibbs free energy change of a reaction. Using thermodynamic arguments (Balmer, 1990), it can be shown that in a chemical reaction such 4-8:

$$\Delta G_f = \Delta G_f^0 - RT \ln\left(\frac{a_J^j a_K^k}{a_M^m}\right) \quad (4-10)$$

where: ΔG_f^0 is the change in Gibbs free energy at standard pressure

In the case of hydrogen fuel cell reaction equation 4-10 becomes:

$$\Delta G_f = \Delta G_f^0 - RT \ln\left(\frac{a_{H_2} a_{O_2}^{\frac{1}{2}}}{a_{H_2O}}\right) \quad (4-11)$$

To see how this equation affects voltage we can substitute into equation 4-7 and obtain:

$$E = \frac{\Delta G_f^0}{2F} - \frac{RT}{2F} \ln\left(\frac{a_{H_2} a_{O_2}^{\frac{1}{2}}}{a_{H_2O}}\right), \text{ or}$$

$$E = E^0 - \frac{RT}{2F} \ln\left(\frac{a_{H_2} a_{O_2}^{\frac{1}{2}}}{a_{H_2O}}\right) \quad (4-12)$$

where: E^0 is the EMF at standard pressure and is a value that we can obtain from table 4.4.

Equation 4-12 is the one that gives the relationship between the theoretical voltage of the hydrogen fuel cell and the concentration and is called Nernst equation.

4.4.3 – Efficiency of PEM fuel cell

The efficiency of a fuel cell is the ratio between the electrical power output and the fuel input (in power units), both of which must be in the same units [W], i.e.

$$\eta_{fc} = \frac{P_{fc}}{F_{in}} \quad (4-13)$$

where: P_{fc} is the electrical power output of the fuel cell and F_{in} is its input fuel (in power units)

The ideal efficiency of a fuel cell could also be given by:

$$\eta_{fc} = \frac{\Delta G}{\Delta H} \quad (4-14)$$

where: ΔG [J/mol] is the change in Gibbs energy that represents the electrical energy output of the fuel cell and ΔH [J/mol] is the reaction enthalpy change which represents the thermal input energy.

The most widely used efficiency value of fuel cells is based on the change in the standard free energy of the cell reaction. In H_2/O_2 PEM fuel cell, the chemical reaction produces water in the liquid form. At STC, the thermal input energy ΔH_0 in the H_2/O_2 reaction is -286 kJ/mol , and the free energy available for useful work is 237.3 kJ/mol . Thus the maximum theoretical H_2/O_2 efficiency is 0.83. In table 4.4 different efficiencies for different values of temperature can be seen:

Form of water product	Temp °C	$\Delta \bar{g}_f$, kJ mol^{-1}	Max EMF V	Efficiency limit %
Liquid	25	-237.2	1.23	83
Liquid	80	-228.2	1.18	80
Gas	100	-225.2	1.17	79
Gas	200	-220.4	1.14	77
Gas	400	-210.3	1.09	74
Gas	600	-199.6	1.04	70
Gas	800	-188.6	0.98	66
Gas	1000	-177.4	0.92	62

Table 4.4: ΔG_f , max EMF and efficiency limit for hydrogen fuel cells

The efficiency of an actual fuel cell stack $\eta_{fc, Stack}$ can be expressed as the ratio of the operating cell voltage (U_{actual}) to the reversible cell voltage (U_{th}). The actual cell voltage is less than the reversible cell voltage because of the losses associated with cell over-voltages, as will be discussed later. Therefore the efficiency of a fuel cell stack can be written as:

$$\eta_{fc, Stack} = 0.83 \frac{U_{actual}}{U_{th}} \quad (4-15)$$

As it can be seen at table 4.4, the reversible cell voltage of a pure H_2/O_2 reaction at reference conditions is 1.23V . Thus the efficiency of a fuel cell stack at reference conditions is given by:

$$\eta_{fc, Stack} = 0.83 \frac{U_{actual}}{U_{th}} = 0.83 \frac{U_{actual}}{1.23} = 0.675xU_{actual} \quad (4-16)$$

A fuel cell can be operated at different current densities. The corresponding cell voltage then determines the fuel cell efficiency. Decreasing the current density increases the cell voltage, thereby increasing the fuel cell efficiency. As the current density is decreased, the active cell area must be increased to obtain the required amount of power. Thus, designing the fuel cell for higher efficiency increases the capital cost, and a trade-off must be made.

4.4.4 – Hydrogen fuel cell consumption

According to Faraday's law, the consumption of hydrogen supplies to a fuel cell is directly proportional to the rate of transfer of electrons at the electrodes, which is equivalent to the output current to the external circuit. Hence, the total hydrogen flow rate consumption to a fuel cell, which consists of several cells connected in series, can be expressed by [Busquet, 2003]:

$$q_{H_2} = \frac{NsI}{nF} x \frac{1}{\eta_f} \quad (4-17)$$

where: q_{H_2} is the hydrogen flow rate, $n = 2$ is the number of electrons per mole, and η_f is Faraday's efficiency.

In an actual PEMFC, hydrogen is usually supplied at flow rates slightly higher than the theoretical maximum value (stoichiometry). This amount of hydrogen reduces the current efficiency, or Faraday's efficiency for the fuel cell. The Faraday's efficiency η_f is defined as the ratio between the theoretical maximum value of hydrogen consumed in the fuel cell and the actual value. Therefore Faraday's efficiency can be calculated from:

$$\eta_f = \frac{q_{H_2, th}}{q_{H_2, actual}} \quad (4-18)$$

where: $q_{H_2, th}$ and $q_{H_2, actual}$ [mol/s] are the theoretical and actual hydrogen flow rate respectively.

4.4.5 - Losses

Figure 4.5 shows the performance of a typical single cell operating at about $70^{\circ}C$, at normal air pressure. The key points to notice about this graph of the cell voltage against current density are as follows:

- Even the open circuit voltage is less than the theoretical value
- There is a rapid initial fall in voltage
- The voltage then falls less rapidly and more linearly
- There is sometimes a higher current density at which the voltage falls more rapidly

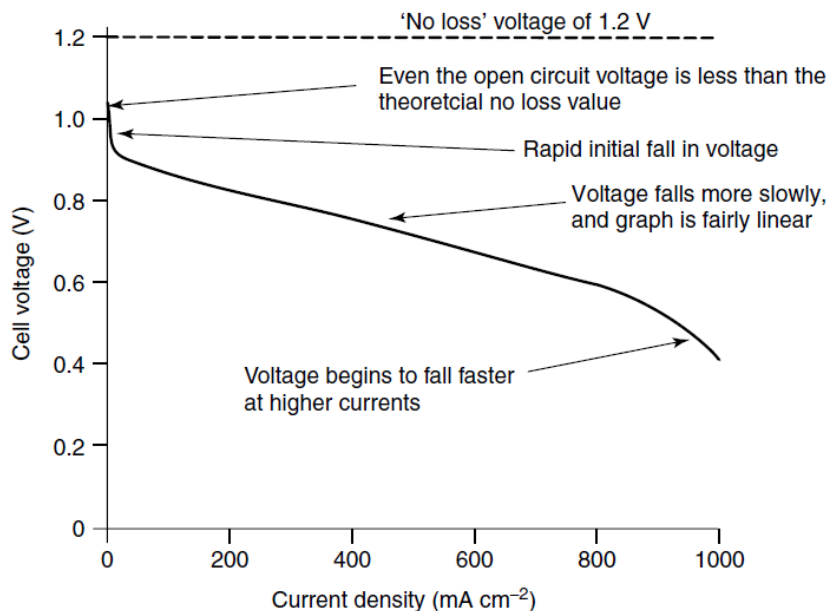


Figure 4.5: Voltage/Current density graph for a low temperature fuel cell

The characteristic shape of the voltage/current density graphs of figure 4.5 results from four major irreversibilities which are discussed in the following sections.

4.4.5.1 – Activation losses

These are caused by the slowness of the reactions taking place on the surface of the electrodes. A proportion of the voltage generated is lost in driving the chemical reaction that transfers the electrons to or from the electrode. Tafel observed in the 1905 that the overvoltage (losses) at the surface of an electrode followed a similar pattern in a great variety of electrochemical reactions. For most values of overvoltage its values is given by the Tafel equation:

$$\Delta V_{act} = A \log\left(\frac{i}{i_0}\right) \quad (4-19)$$

where: i is the current density, i_0 is the exchange current density and A is a constant.

In the case of hydrogen fuel cell A is given by the formula:

$$A = \frac{RT}{2aF} \quad (4-20)$$

In formula 4-20 a is the charge transfer coefficient, which is the proportion of the electrical energy applied that is harnessed in changing the rate of an electrochemical reaction. Its value depends on the reaction involved and the material the electrode is made from, but it must be in the range of 0 to 1. For the hydrogen electrode its value is about 0.5 for a great variety of electrode materials.

The appearance of T in formula 4-20 can give the impression that raising the temperature increases the overvoltage. This is very rarely the case, as the effect of increases in i_0 with temperature far outweigh any increase in A . The key to making the activation overvoltage as low as possible is this i_0 , which can vary by several orders of magnitude. The smaller the i_0 , the greater the voltage drop. In Table 4.5 different values of i_0 can be seen for various electrode materials.

Metal	i_0 (A cm ⁻²)
Pb	2.5×10^{-13}
Zn	3×10^{-11}
Ag	4×10^{-7}
Ni	6×10^{-6}
Pt	5×10^{-4}
Pd	4×10^{-3}

Table 4.5: i_0 for several electrode materials for acid electrolyte

There are many ways to increase the exchange current density, thus decreasing the activation overvoltage and improving the fuel cell performance:

- Using more effective catalysts
- Increasing the roughness of the electrodes. This increases the real surface area of each nominal 1cm^2 , and this increases i_0 .
- Increasing reactant concentration, for example using pure oxygen instead of air. This works because the catalyst sites are more effectively occupied by reactants.
- Increasing the pressure. This is also presumed to work by increasing catalyst site occupancy

Another important comment is that the Tafel equation is true only if $i > i_0$.

4.4.5.2 – Fuel crossover and internal currents

This energy loss results from the waste of fuel passing through the electrolyte, and, to a lesser extent, from the electron conduction through the electrolyte. The electrolyte should only transport ions through the cell. However a certain amount of fuel diffusion and electron flow will always be possible. Internal currents are not easy to measure, so the modeling of this overvoltage is usually done by adding the internal current i_n to equation 4-19:

$$\Delta V_{act} = A \log\left(\frac{i + i_n}{i_0}\right) \quad (4-20)$$

In general the internal current and/or diffusion of hydrogen through the electrolyte of a fuel cell is not usually of great importance in terms of efficiency. However, in the case of low temperature cells, it has a very marked effect on the open circuit voltage.

4.4.5.3 – Ohmic losses

These are the losses due to the electrical resistance of the electrodes, and the resistance to the flow of ions through the electrolyte. The size of the voltage loss is simply proportional to the current:

$$\Delta V = IR \quad (4-21)$$

Three ways for reducing the internal resistance of the cell are as follows:

- The use of electrodes with the highest possible conductivity
- Good design and use of appropriate materials for the bipolar plates or cell interconnects
- Making the electrolyte as thin as possible

4.4.5.4 – Concentration losses

These result from the change in concentration of the reactants at the surface of the electrodes as the fuel is used. It is normal that the hydrogen concentration decreases as it flows through the electrode and the same stands for the concentration of oxygen. So there is a pressure drop for both the hydrogen and the oxygen. This reduction in gas pressure results in a reduction in voltage. However, it is generally agreed among fuel cell researchers that there is no analytical solution to the problem of modeling the changes in voltage that works satisfactorily in all cases [Kim et al.,1995].

4.5 – Simulink modeling of PEMFC

At this section the Simulink models implementing the formulas discussed in the previous section will be presented. At figure 4.6 the block of the Fuel Cell Subsystem can be seen:

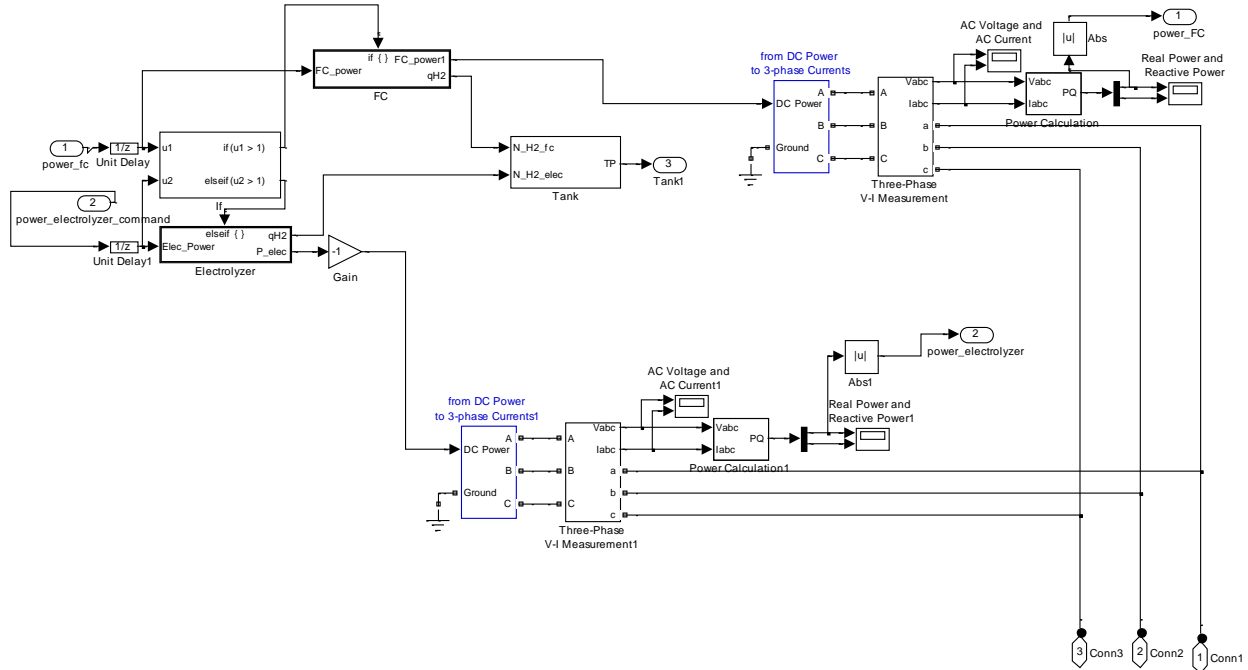


Figure 4.6 : Fuel Cell Subsystem

The inputs of this block are:

- $power_fc$: This is the power the fuel cell has to provide to the system if the solar power is not enough to meet the needs.
- $power_electrolyzer_command$: This is the power which will be stored in hydrogen by the electrolyser.

The outputs of this block are:

- $power_FC$: This is the power produced by the fuel cell
- $power_electrolyzer$: Power used by the electrolyser
- $Tank1$: This is the pressure of hydrogen in the Tank, where it is stored
- $Conn1, Conn2, Conn3$: These are the connections with the house grid

At the beginning of the block there is an if-block which decides whether the Fuel Cell or the electrolyser will be working. These two system components cannot be working together according to our controller. The power from the Fuel Cell, as well as the power consumed by the electrolyser, are converted to 3-phase currents at the components provided by Simulink, as it is obvious in figure 4.7.

4.5.1 – Fuel Cell Stack

In figure 4.7 the block of the Fuel Cell Stack can be seen:

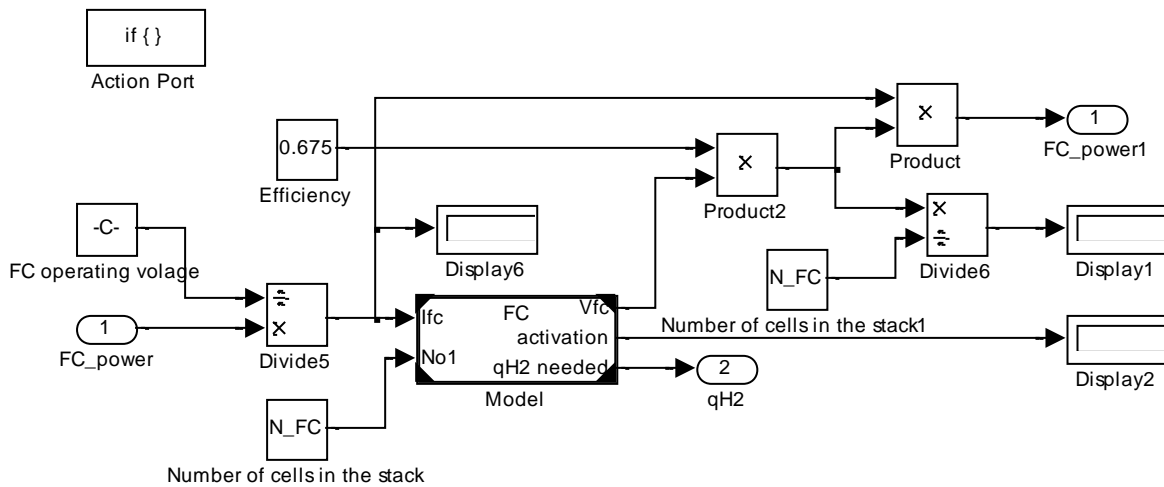


Figure 4.7: Fuel Cell Stack

The input of this block is FC_power , which is the power the Fuel Cell Stack has to provide. This power is then divided by $FC_operating_voltage$, which is the operating voltage of the stack, taken by the datasheet of the unit, in order to estimate the current that will be flowing through the stack. This block also contains the fuel cell block, which is the Simulink model for a single fuel cell and will be discussed later. The output voltage of the fuel cell is multiplied with the efficiency of the stack, corresponding to formula 4-16, and, then, it is multiplied by N_FC , which is the number of cells in a fuel cell stack (75 in our case).

The outputs of this system are:

- FC_power1 : This is the power the fuel cell stack provides to the system
- $qH2$: This is the hydrogen flow that must be provided to the cell in order to provide the necessary power

4.5.2 – Fuel Cell

In figure 4.8 the fuel cell block can be seen:

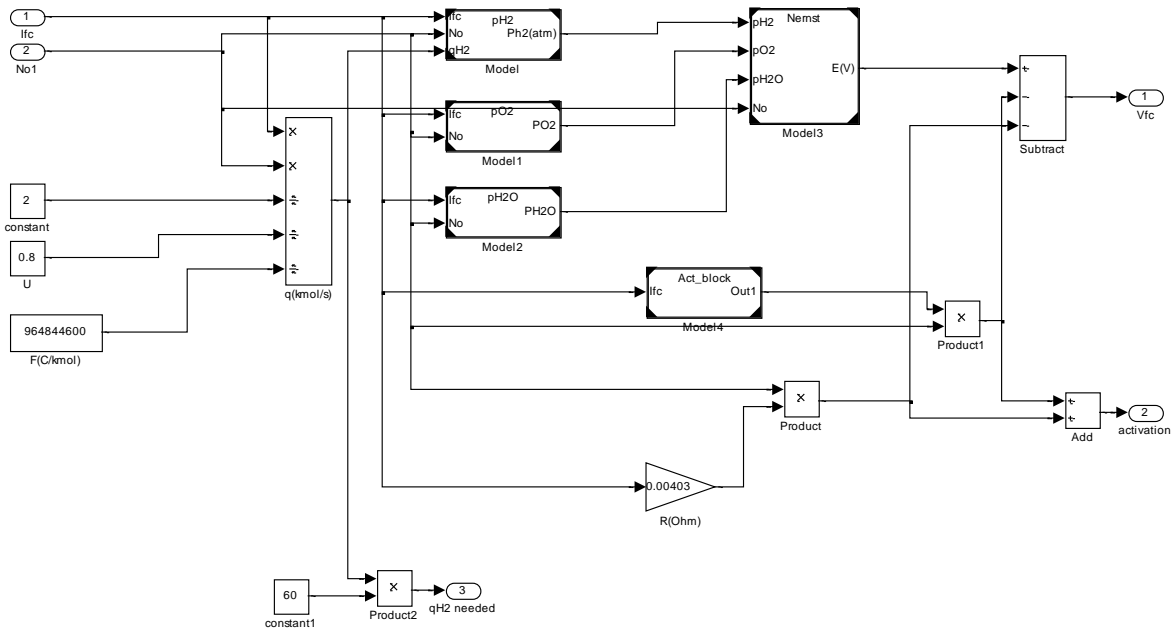


Figure 4.8: Fuel Cell

The inputs of this block are:

- I_{fc} : This is the current flowing through the fuel cell
- $No1$: This is the number of fuel cells in the stack

First the amount of hydrogen moles per second needed by the stack is estimated by the divider $q(kmol/s)$, which corresponds to formula 4-17. Faraday's efficiency, η_f , in our case is 0.8. Then the pressures of hydrogen, oxygen and water of the fuel cell are estimated in the blocks $pH2$, $pO2$, $pH2O$ respectively. These blocks will be discussed later. These pressures are needed for the estimation of the actual fuel cell voltage, which is done in the *Nernst* block. Finally two kind of losses are subtracted by the actual fuel cell voltage – activation losses and Ohmic losses.

The outputs of this block are:

- V_{fc} : This is the actual fuel cell voltage
- *activation*: This is the activation losses

It should be noted that the hydrogen flow estimated according to formula 4-17 is then multiplied by 60, as we need the hydrogen flow per minute and the formula estimates the hydrogen flow per second.

A constant operating temperature of 323K is assumed.

4.5.2.1 – Operating Pressure in the fuel cell stack

In figure 4.9 the block where the calculation of the operating pressure of the hydrogen is done, can be seen:

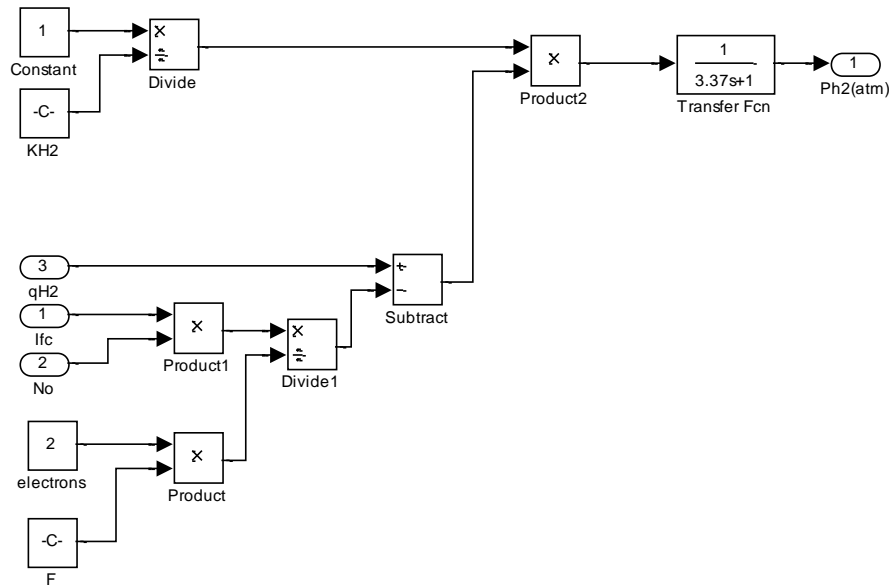


Figure 4.9: Hydrogen pressure

The inputs of this block are:

- q_{H2} : This is the hydrogen flow in the fuel cell
- I_{fc} : This is the current flowing through the fuel cell
- No : This is the number of fuel cells in the stack

The calculation of the pressure of hydrogen is being done according to the formula:

$$p_{H_2} = \frac{1/K_{H_2}}{1 + \tau_{H_2} s} (q_{H_2_in} - q_{H_2_out}), \text{ where } \tau_{H_2} = \frac{V_a}{K_{H_2} RT} [s] \text{ and } q_{H_2} = \frac{I}{2F}$$

- where:
- K_{H_2} is the hydrogen valve molar constant, $4.7955 \cdot 10^{-7} [\text{kmol}/\text{atm} \cdot \text{s}]$
 - τ_{H_2} is hydrogen time constant, 3.37 s
 - $q_{H_2_in}$ is the hydrogen flow in the fuel cell

- $q_{H_2_out}$ is the hydrogen reacting in the fuel cell

The output of this block is the operating pressure of hydrogen.

In figure 4.10 the block where the calculation of the operating pressure of the oxygen is done, can be seen:

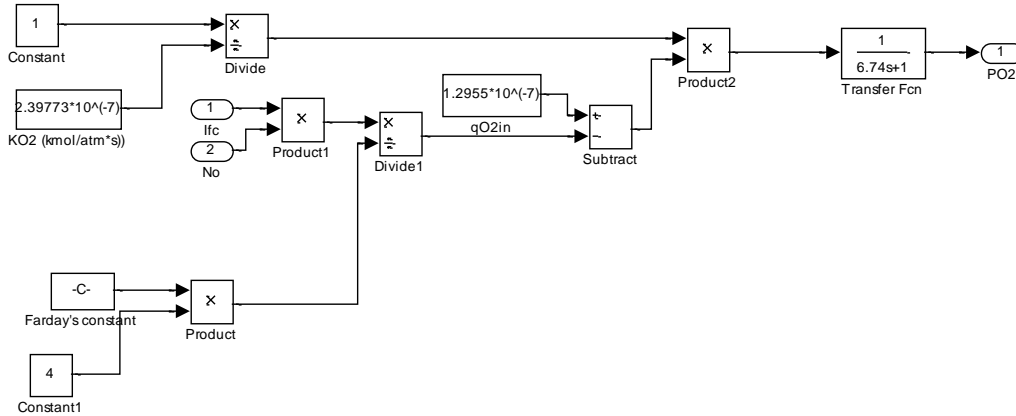


Figure 4.10: Pressure of oxygen

The inputs of this block are:

- I_{fc} : This is the current flowing through the fuel cell
- No : This is the number of fuel cells in the stack

The calculation of the pressure of oxygen is being done according to the formula:

$$p_{O_2} = \frac{1/K_{O_2}}{1 + \tau_{O_2} s} (q_{O_2_in} - q_{O_2_out}), \text{ where } \tau_{O_2} = \frac{V_c}{K_{O_2} RT} [s] \text{ and } q_{O_2} = \frac{1}{2} \frac{I}{2F}$$

where: - K_{O_2} is the oxygen valve molar constant, $2.39773 \cdot 10^{-7} [\text{kmol/atm} \cdot \text{s}]$

- τ_{O_2} is hydrogen time constant, $6.74s$
- $q_{O_2_in}$ is the hydrogen flow in the fuel cell
- $q_{O_2_out}$ is the hydrogen reacting in the fuel cell

It should be noted that $q_{O_2_in}$ was assumed to be $1.2955 \cdot 10^{-7}$ moles/s.

The output of the block is the operating system of oxygen.

In figure 4.11 the block where the calculation of the operating pressure of water is done, can be seen:

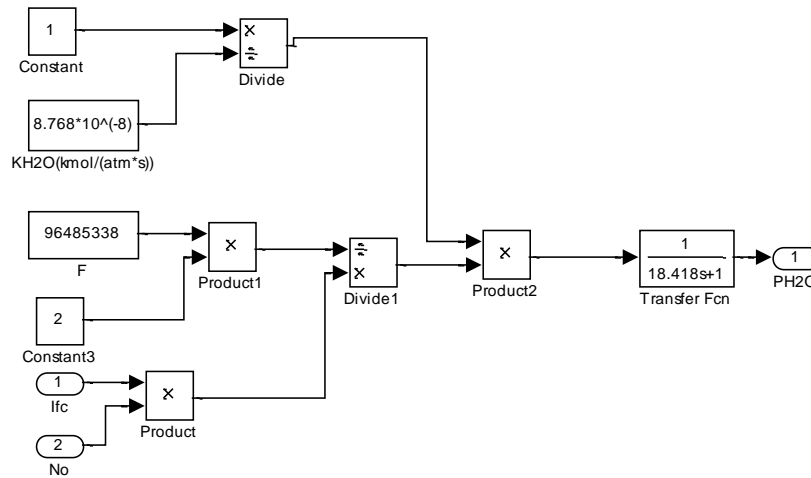


Figure 4.11: Pressure of water

The inputs of this block are:

- I_{fc} : This is the current flowing through the fuel cell
- No : This is the number of fuel cells in the stack

The calculation of the pressure of oxygen is being done according to the formula:

$$p_{H_2O} = \frac{1/K_{H_2O}}{1 + \tau_{H_2O} S} (q_{H_2O_in} - q_{H_2O_out}), \text{ where } \tau_{H_2O} = \frac{V_c}{K_{H_2O} R T} [s] \text{ and } q_{H_2O} = -\frac{I}{2F}$$

where: - K_{H_2O} is the oxygen valve molar constant, $8.768 \cdot 10^{-8} [\text{kmol}/\text{atm} \cdot \text{s}]$

- τ_{H_2O} is hydrogen time constant, $18.418s$
- $q_{H_2O_in}$ is the hydrogen flow in the fuel cell
- $q_{H_2O_out}$ is the hydrogen reacting in the fuel cell

The output of this block is the operating pressure of the water.

4.5.2.2 – Nernst equation

In figure 4.12 the block where the calculation of the theoretical voltage of the fuel cell stack, without the losses, can be seen:

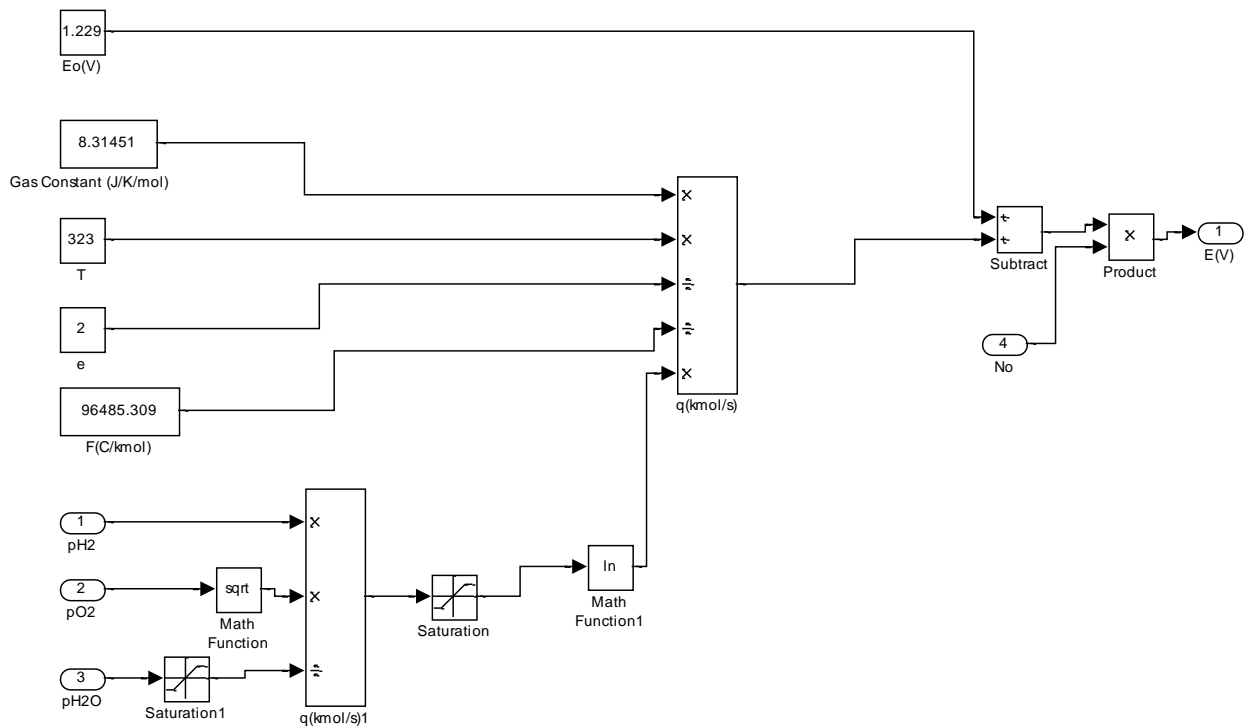


Figure 4.12: Nernst equation

The inputs of this block are:

- p_{H_2} : The operating pressure of hydrogen
- p_{O_2} : The operating pressure of oxygen
- p_{H_2O} : The operating pressure of water

This block is the implementation of Nernst equation, given in formula 4-12:

$$E = E^0 - \frac{RT}{2F} \ln\left(\frac{P_{H_2} P_{O_2}^{\frac{1}{2}}}{P_{H_2O}}\right)$$

It must be noted that after the estimation of the theoretical fuel cell voltage, it is multiplied with the number of fuel cells in the stack in order to estimate the theoretical fuel cell voltage of the whole stack, which is the output of this block.

4.5.2.3 – Losses

In this section the Simulink blocks that implement the formulas for the voltages losses in the stack will be discussed. Only activation losses and Ohmic losses were modeled as fuel crossover and internal current losses are negligible, and the estimation of concentration losses has no analytical solution, as mentioned in section 4.4.5.4.

In figure 4.13 the block where the estimation of activation losses is being done can be seen:

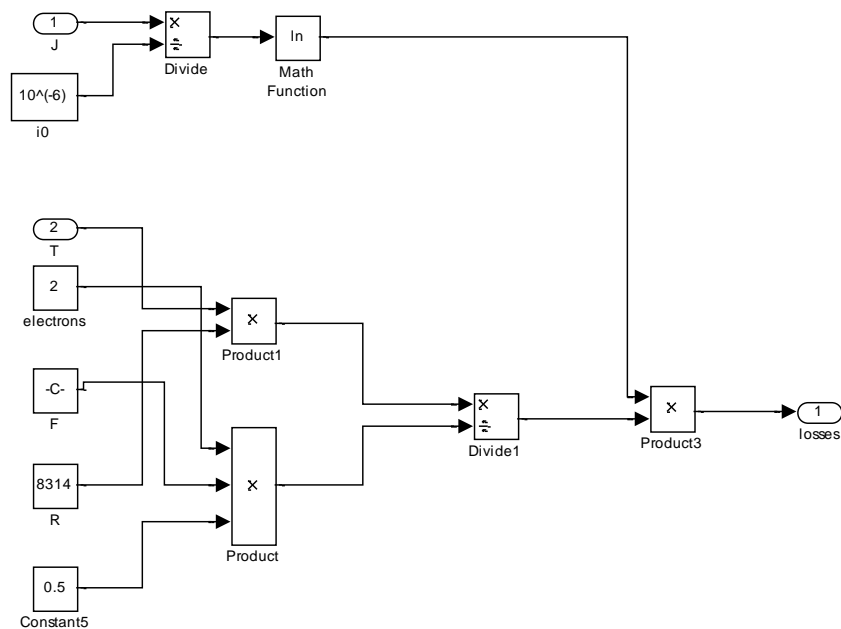


Figure 4.13: Activation losses

The inputs of this block are:

- J : This is the current density in the fuel cell
- T : This is the operating temperature of the cell

This block is the implementation of Tafel equation, which is given in formula 4-19:

$$\Delta V_{act} = A \log\left(\frac{i}{i_0}\right)$$

It should be noted that an exchange current density of :

$$i_0 = 10^{(-6)} \text{A/cm}^{-2} \text{ was assumed.}$$

The output of this block is the activation losses for one fuel cell.

The Ohmic losses were modeled according to formula 4-21, with an internal resistance of 0.00403Ω , found in literature survey. For the modeling a Gain block was used, meaning that the current flowing through the cell is multiplied with the internal resistance of one cell, and then multiplied with the number of cells in the stack, giving in the end the Ohmic losses. Finally the Ohmic losses are subtracted by the theoretical voltage of the fuel cell stack.

4.5.3 – Electrolyser

According to Faraday's law, hydrogen production rate of an electrolyser cell is directly proportional to the electrical current in the equivalent electrolyser circuit, and is given by the formula:

$$q_{H_2} = \frac{\eta_f N_e i_e}{2F} \quad (4-22)$$

where: - q_{H_2} is the produced hydrogen (*moles / s*)

- η_f is Faraday's efficiency
- N_e is the number of cells of the electrolyzer
- i_e is the current flowing through the electrolyser
- F is Faraday's constant

Assuming that the working temperature of the electrolyser is $40^\circ C$, Faraday's efficiency is given by the following formula:

$$\eta_f = 96.5e^{(0.09/i_e - 75.5/i_e^2)} \quad (4-23)$$

In figure 4.14 the implementation of formula 4-22 can be seen:

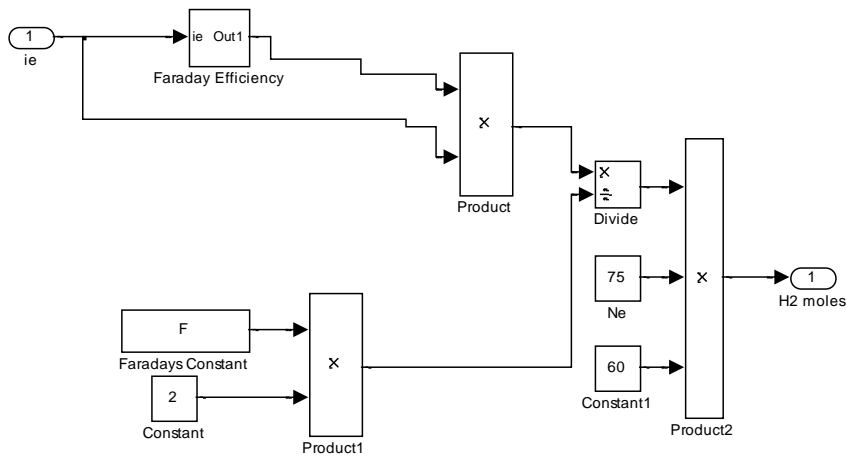


Figure 4.14: Faraday's law

The input of this block is i_e , which is the current flowing through the electrolyser. The hydrogen produced according to the formula is multiplied by 60, as output of the system must be the hydrogen produced per minute and not per second.

The Simulink model which calculates the Faraday's efficiency, according to formula 4-23 can be seen in figure 4.15:

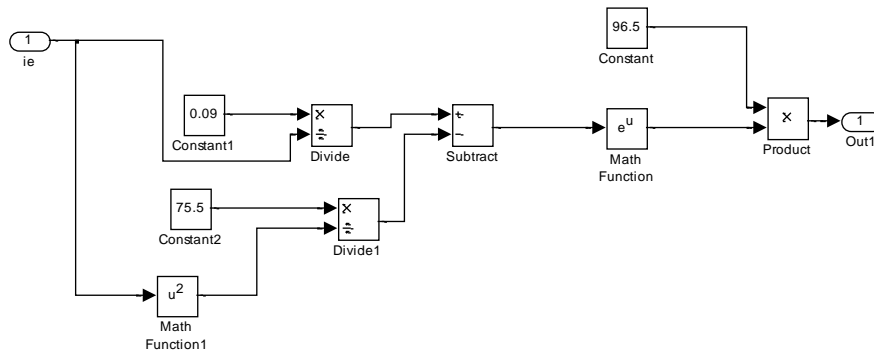


Figure 4.15: Faraday's efficiency

4.5.4 – Storage

The hydrogen storage technique used in the system is physical hydrogen storage which involves using a tank for storing hydrogen gas. The hydrogen storage model directly calculates the tank pressure using the ratio of hydrogen flow to the tank and is based on the following formula:

$$P_b - P_{bi} = z \frac{q_{H_2} R T_b}{M_{H_2} V_b} \quad (4-24)$$

where: - P_b is the tank pressure [Pa]

- P_{bi} is the initial tank pressure [Pa]

- q_{H_2} is the hydrogen flow in/out of the tank [moles/s]

- T_b is the operating flow of the tank, 313K

- M_{H_2} is the molecular mass of hydrogen [2gr/mol]

- V_b is the volume of the tank [L]

The Simulink model of the system has an initial pressure of 50atm and a volume of $1m^3$. It can be seen in figure 4.16:

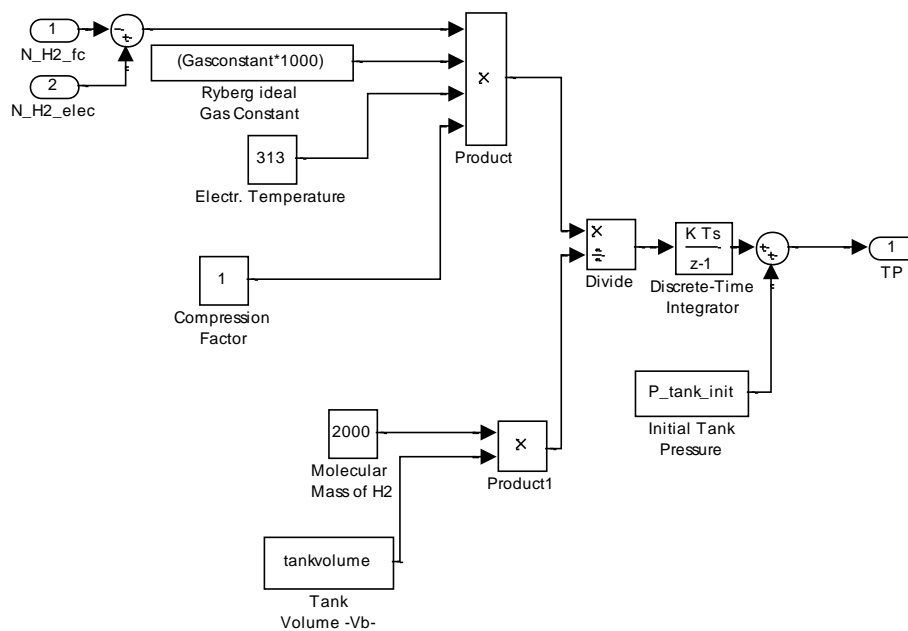


Figure 4.16: Tank

The inputs of this block are:

- N_H2_fc , which is the hydrogen required by the fuel cell
- N_H2_elec , which is the hydrogen produced by the electrolyser.

The output of this block is the pressure of the Tank.

Chapter 5 – Simulation Results

In this section the results of the Simulink simulation will be discussed.

5.1 - Data

For the simulation of the system data were gathered for the solar irradiation and the temperature for the duration of one year for the city of Chania, which is the location of the stand-alone power plant discussed in this thesis. 3 model days were picked, one winter day, one summer day and one spring day. In that way the system is checked for different conditions, extreme, such as summer and winter days and medium, such as the spring day. The simulation is for the duration of one day each time, as longer simulations were impossible with the computer system used.

In Figure 5.1 the temperature at the city of Chania for the first of January is shown:

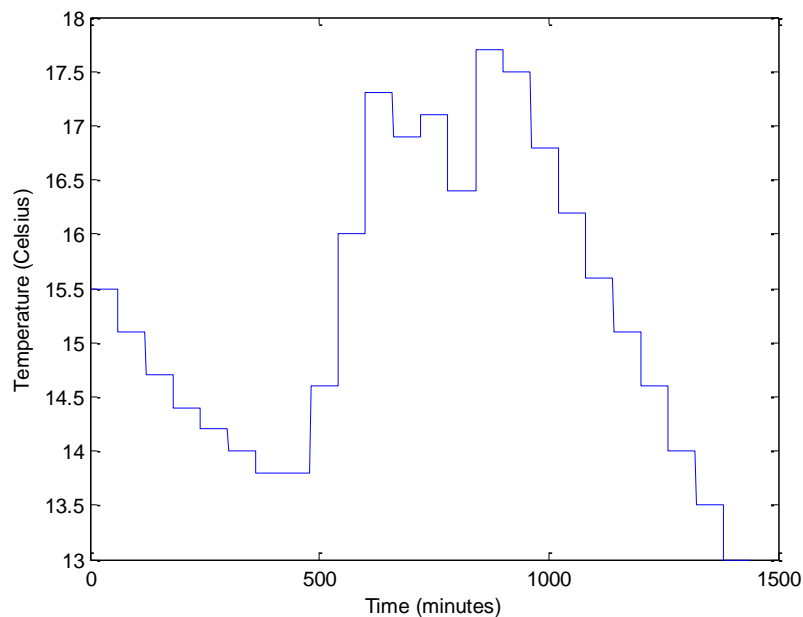


Figure 5.1: 1st of January – temperature

It must be noted here that the only available data about temperature and irradiation for the city of Chania were per hour. Since the simulation is per minute, it is logical for the graphs of temperature and irradiation not to present variations with a high frequency, but in the way shown in the figures.

The irradiation for the same day is shown in Figure 5.2 below:

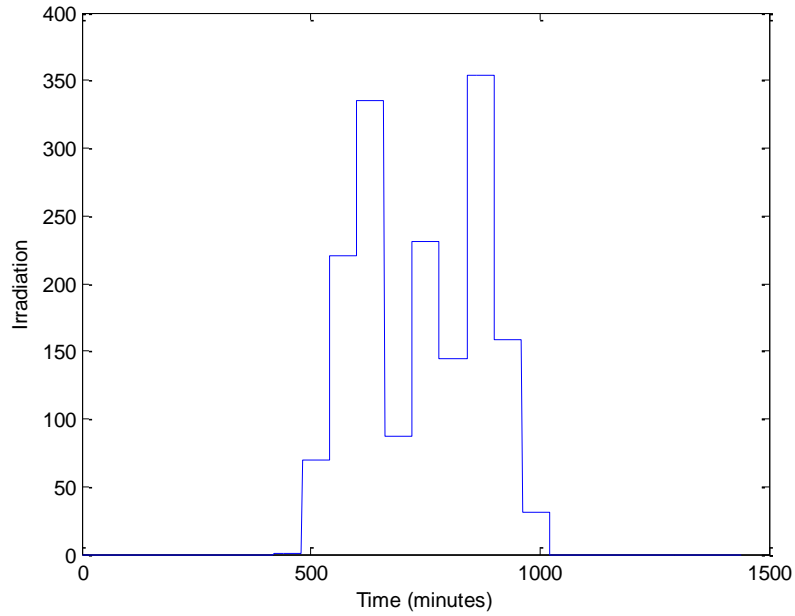


Figure 5.2: 1st of January - Irradiation

As it can be seen from this graph (5.2), the irradiation during winter time is relatively low.

Finally in figure 5.3 the load for one household for the duration of a day is presented:

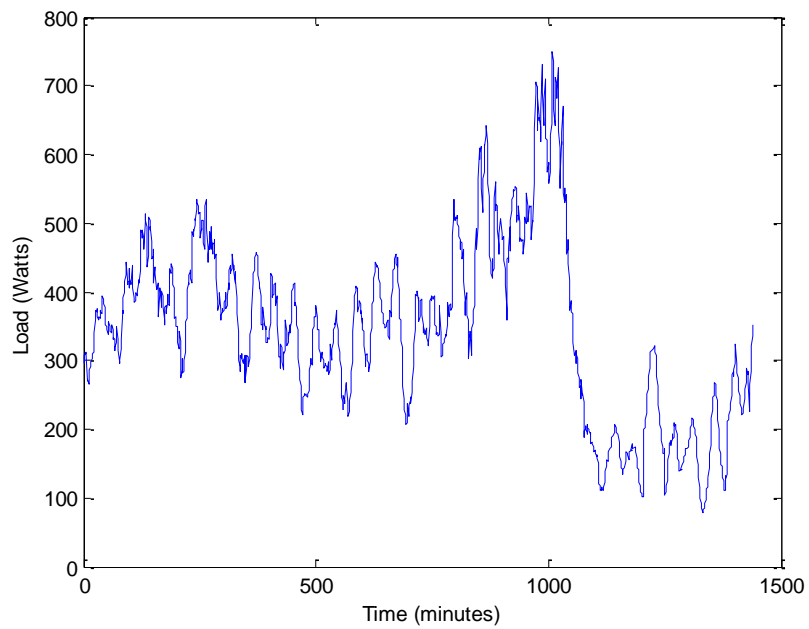


Figure 5.3: Load of one household for one day

The load remains the same for every experiment. In Figure 5.4, the temperature of the 1st of April can be seen:

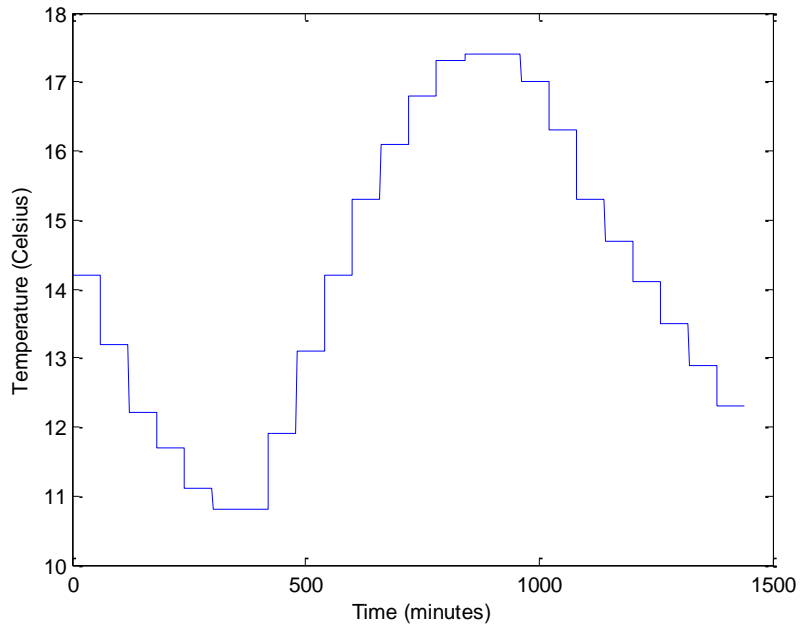


Figure 5.4: 1st of April – Temperature

In Figure 5.5, the irradiation for the 1st of April can be seen:

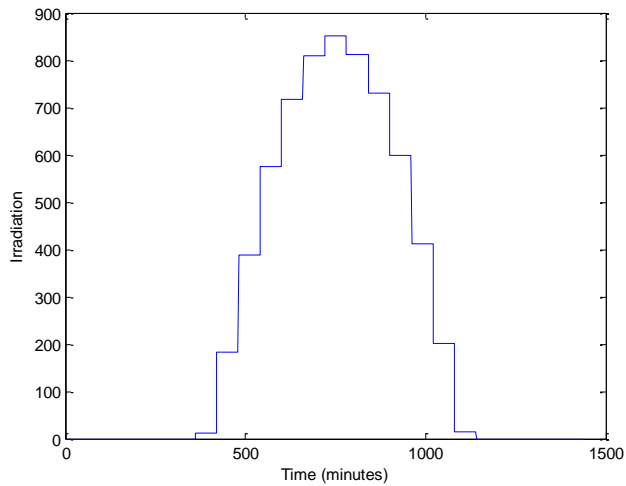


Figure 5.5: 1st of April – Irradiation

Finally in Figure 5.6 the temperature at the first of July at the city of Chania can be seen:

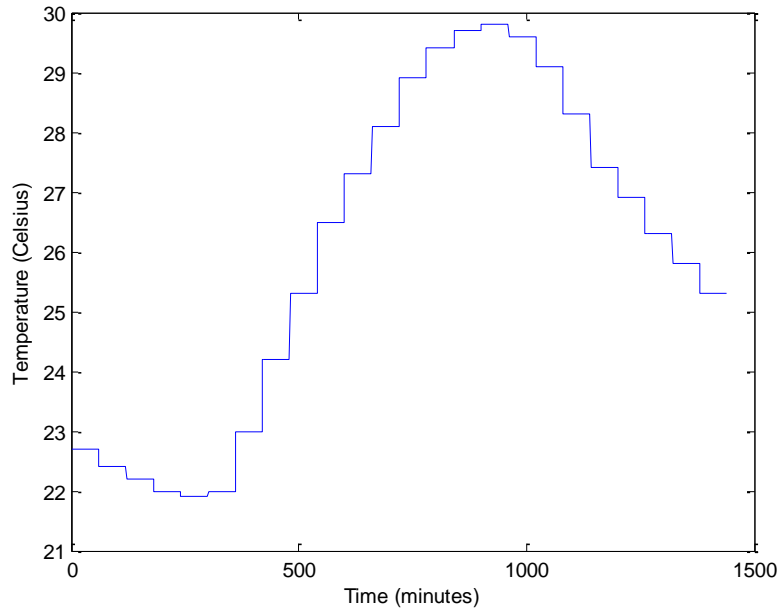


Figure 5.6: 1st of July – Temperature

And in Figure 5.7 the irradiation at the first of July can be seen:

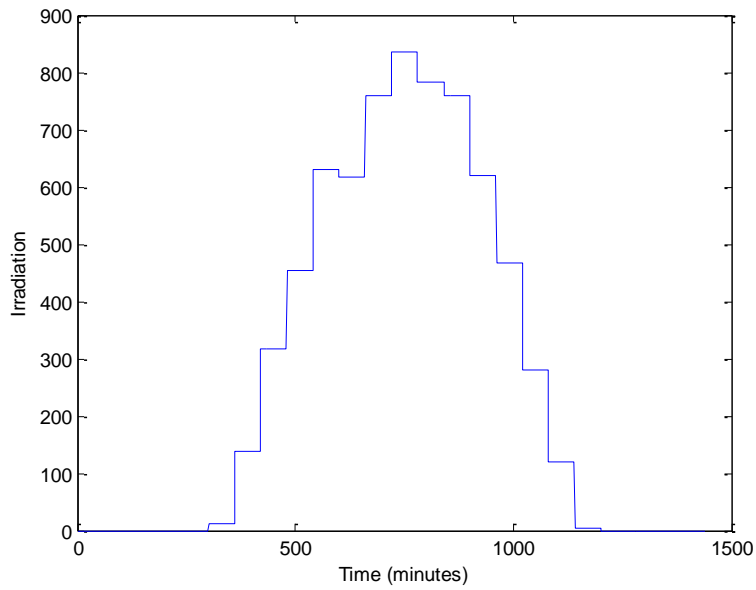


Figure 5.7: 1st of July – Irradiation

5.2 – System Performance

The performance of the system studied will be checked under the conditions derived from the data above and under special cases that may not occur under these conditions.

5.2.1 – Winter day

In Figure 5.8 the power produced by the 7 photovoltaic modules of the system can be seen:

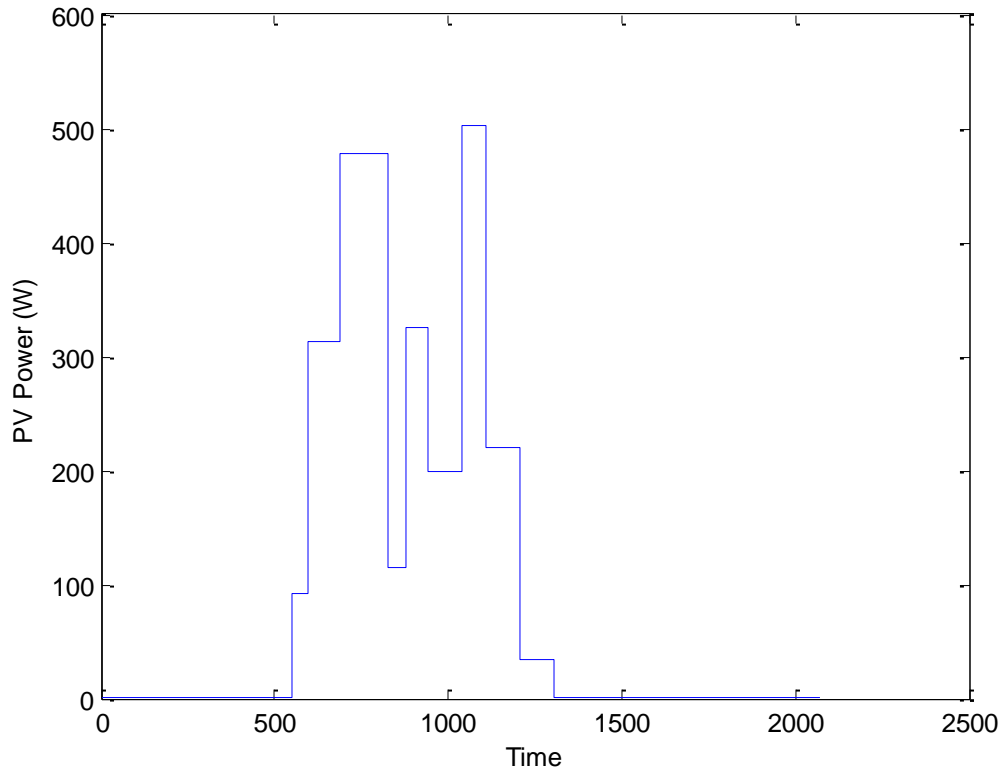


Figure 5.8: PV generator power for winter day

It is obvious that during the winter the PV generator does not produce enough power, mostly due to the very low irradiation at the time. The temperature is also lower than the summer, but it is still a high temperature compared to the one of the tested conditions.

In Figure 5.9 the plot of the PV power and the load can be seen:

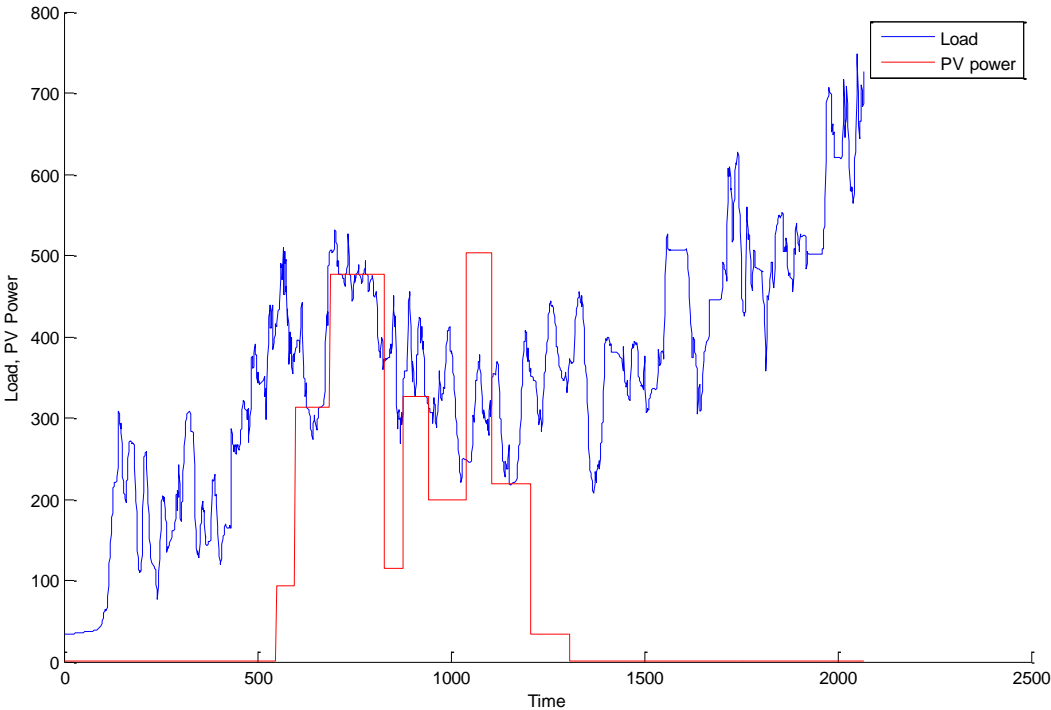


Figure 5.9: PV power and Load for 1st of January

It is obvious that the power produced by the photovoltaic generator is not enough to produce the necessary power for the stand-alone system, so the fuel cell stack has to produce the difference.

In Figure 5.10 the difference in power between the load and the power produced by the PV generator can be seen:

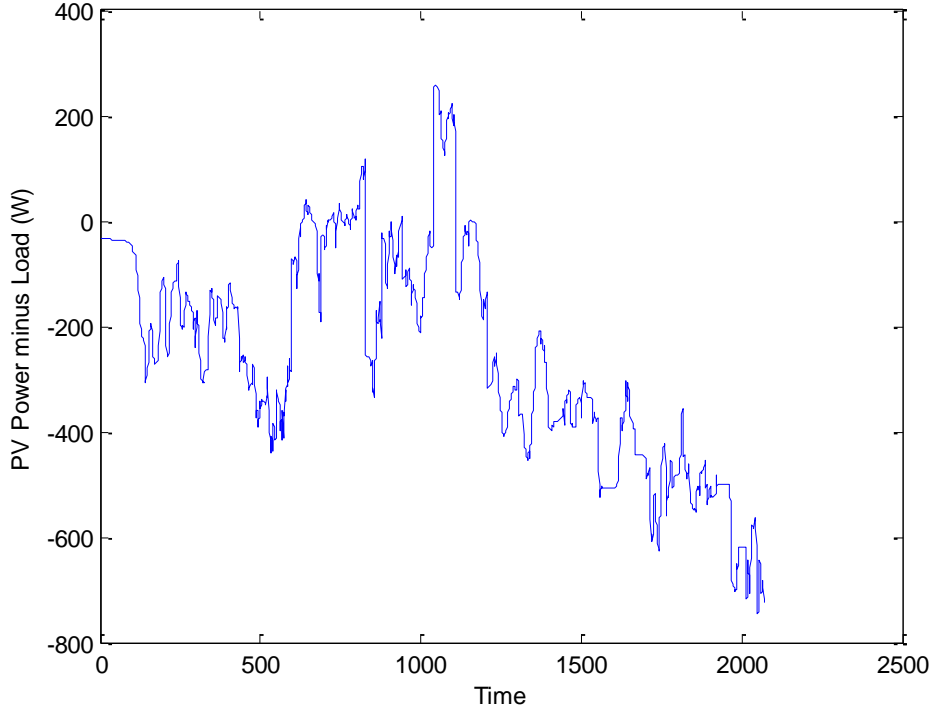


Figure 5.10: Difference between PV Power and Load

Only during daytime the PV generator can produce enough power to cover the load. Again, that is expected considering the weather conditions which are suitable for photovoltaic energy generation.

In figure 5.11 the power produced by the fuel cell, the load and the PV power can be seen:

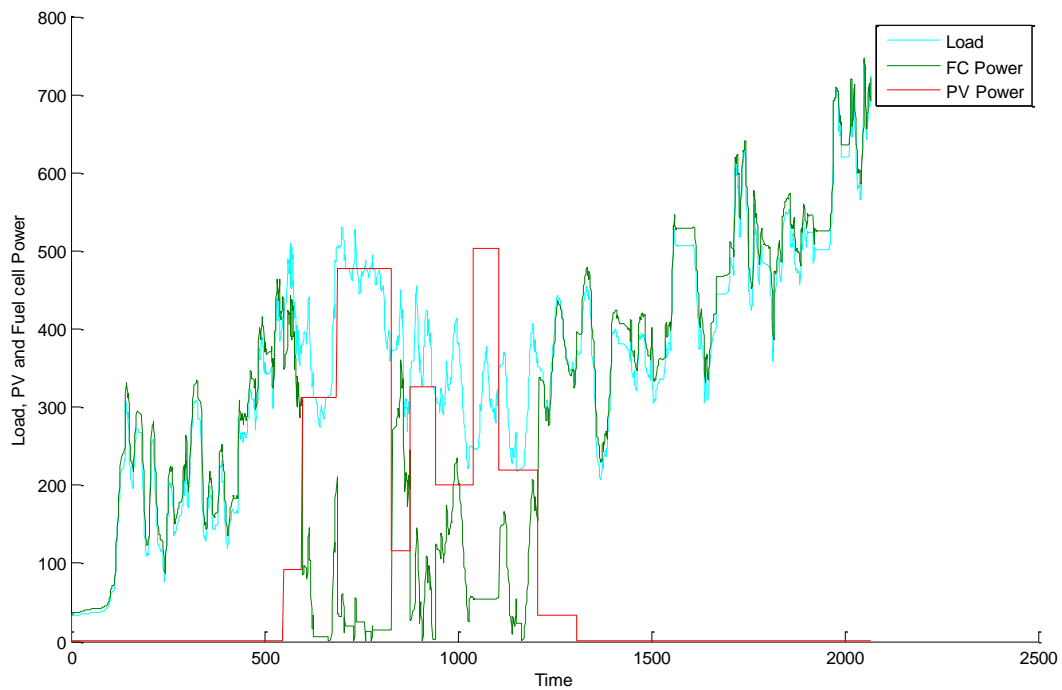


Figure 5.11: FC power, PV power and load

The fuel cell responds well to the energy needs of the system and it is obvious that the controller works efficiently, as the results in this graph are as expected. That means that the fuel cell operates during night hours, providing power for the system, and also provides the power shortage during the day. This is normal, as it has a rated power of 1KW, which is more than the load.

In Figure 5.12, the use of the extra energy produced by the PV generator is used in order to charge the battery:

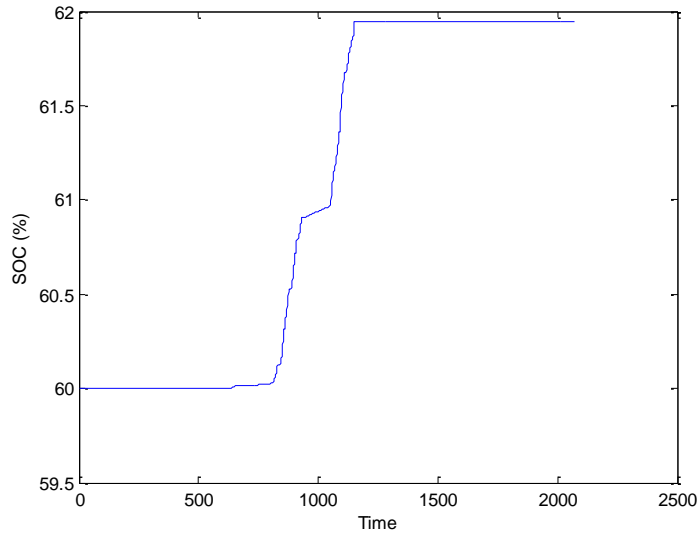


Figure 5.12: SOC for 1st of January

Of course the battery is charged only when the PV generator provides power. Finally in Figure 5.13 the tank empties because of the use of the fuel cell:

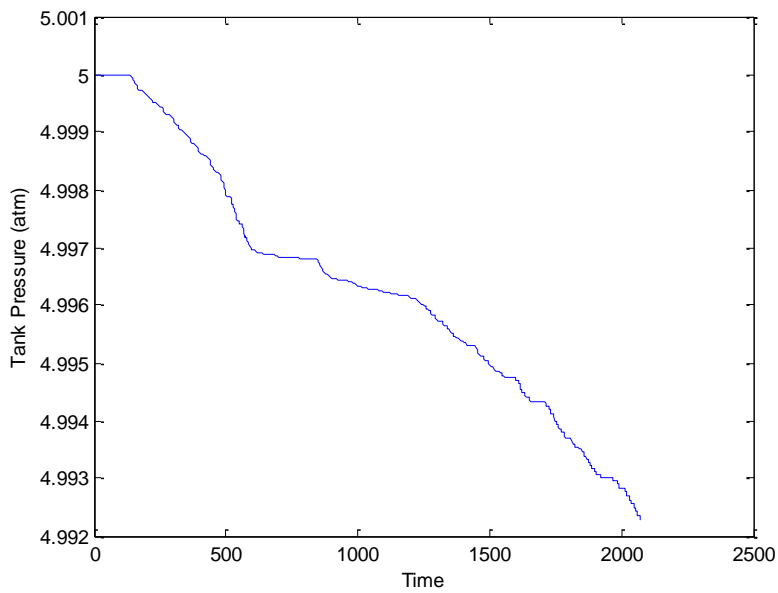


Figure 5.13: 1st of January – Tank pressure

5.2.2 – Spring day

In Figure 5.14 the power produced by the PV generator can be seen:

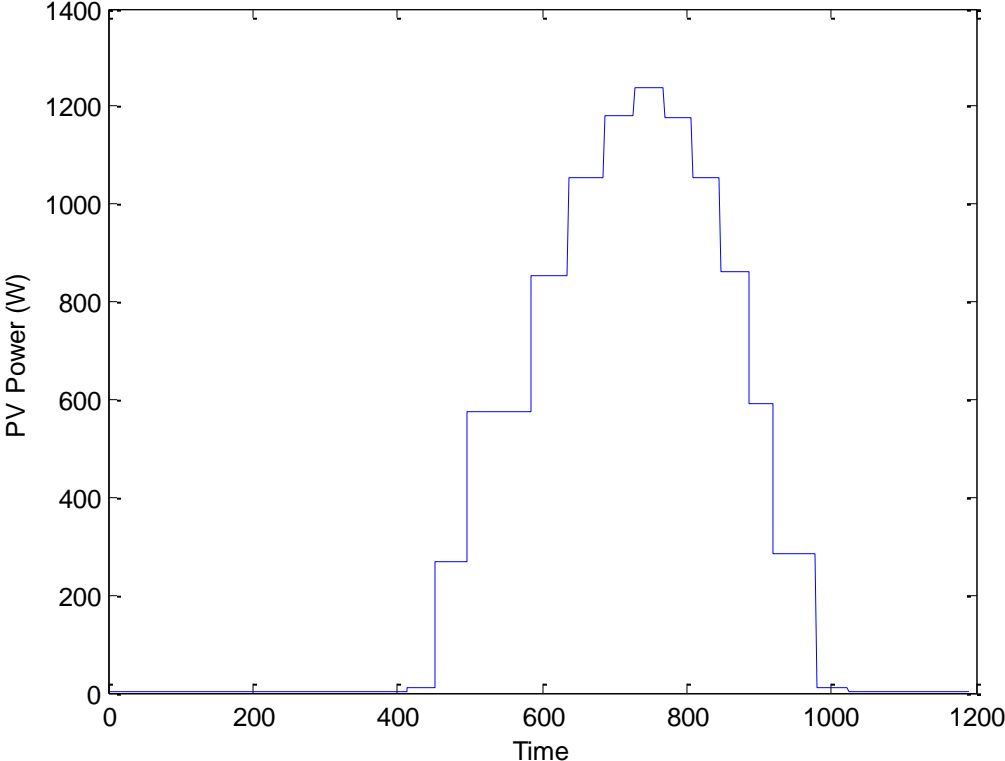


Figure 5.14: PV power for 1st of April

At the spring day the PV generator produces more than double the power it produced during the winter, due to the increment in irradiation and temperature.

In Figure 5.15 the PV power is shown in the same plot with the current, in order to observe their behavior:

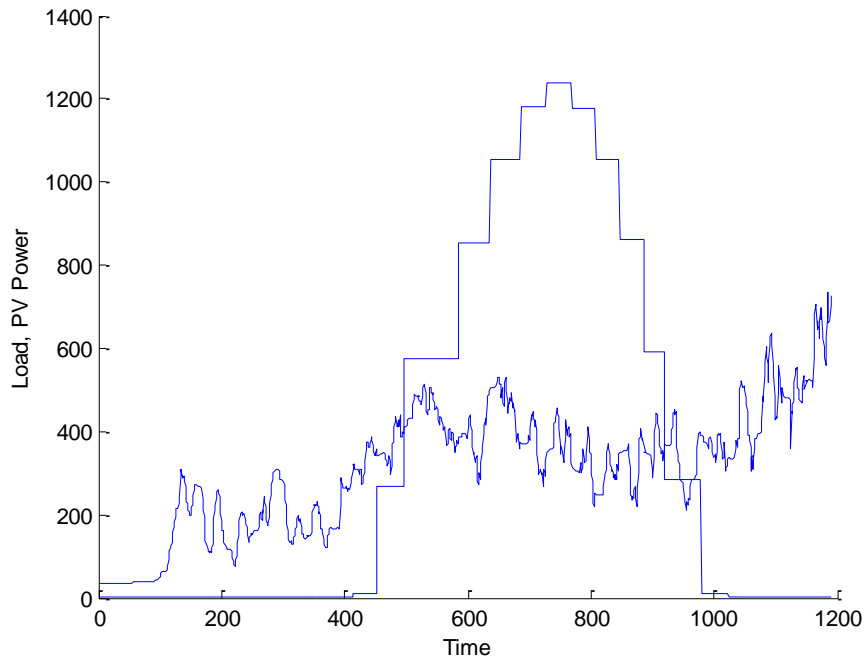


Figure 5.15: PV Power and Load for 1st of April

The PV generator produces a large amount of surplus power which, judging from the graph may be able to storage enough power during the day to cover the power shortage during the night hours. This is very good for the system studied, as spring was taken as a “mean” case, when no important energy losses or gains would be possible.

In Figure 5.16 the difference between the PV power and the Load is shown:

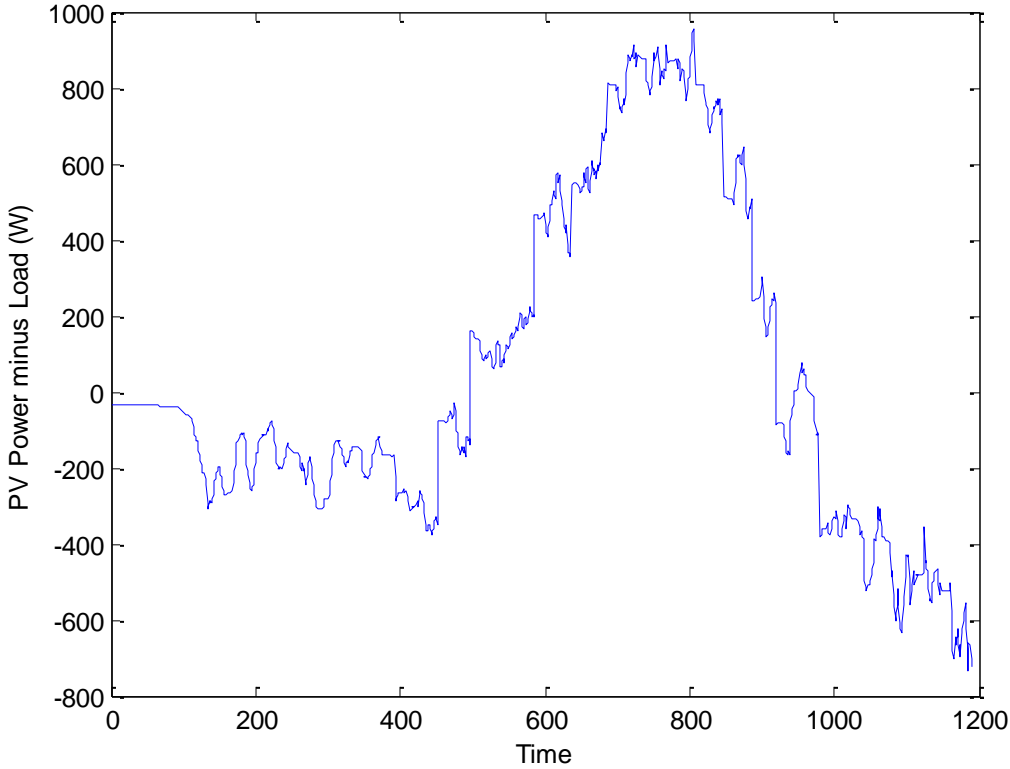


Figure 5.16: Difference between load and PV power for 1st April

More or less the same conclusions can be drawn from this graph as from the previous one.

In Figure 5.17 the relationship between the PV power, the FC power and the Load is shown:

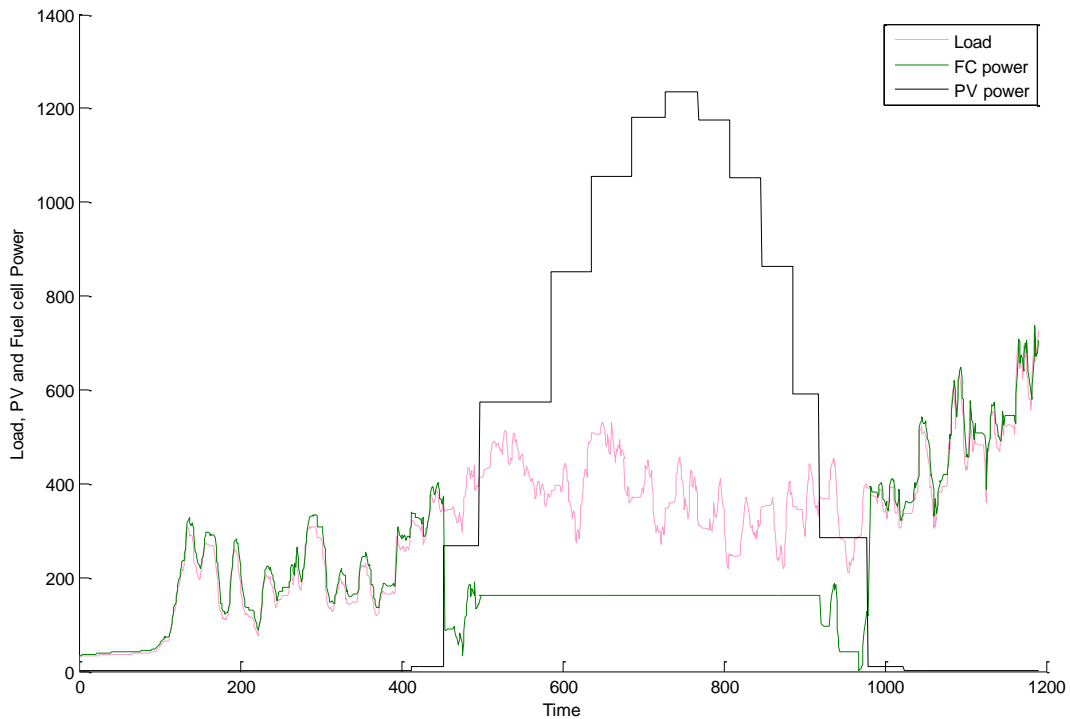


Figure 5.17: PV and FC power – Load for 1st April

The important thing in this graph is that the fuel cell does not fall to zero when there is power surplus from the PV generator. This happens because of the low accuracy of the solver chosen for the Simulink simulation. The proposition for the usage of this particular solver was made by Matlab, as the previous solver used produced some very unusual results. The controller of the system works fine, as it was shown in the Figure 5.12.

The behavior of the battery remains the same, as shown in Figure 5.18:

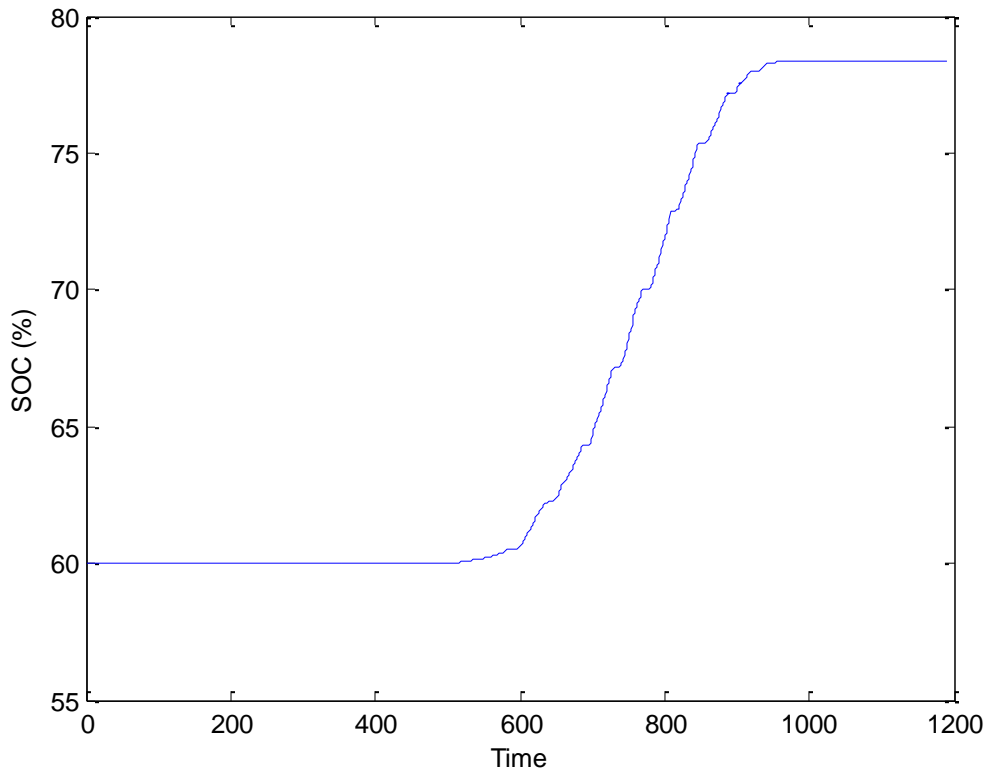


Figure 5.18: SOC for 1st of April

It is important to note that there was a 25% increase in the battery state of charge, only by one day of power surplus by the system. That is normal, because battery is not the main power storage of the system, but it exists for extreme cases and to assure the continuous voltage regulation.

Finally in Figure 5.19 the behavior of the tank is found the same as in the winter day, as the power surplus of the photovoltaic generator is used for charging the battery.

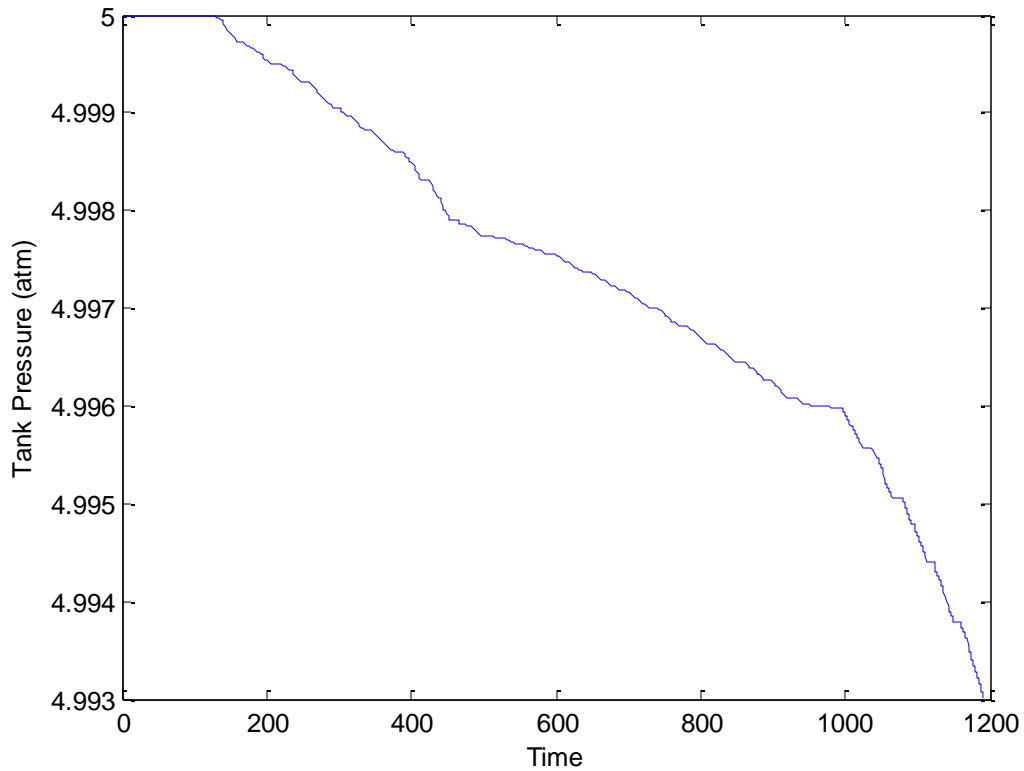


Figure 5.19: Tank pressure for 1st of April

It can be seen that there is not significant loss of pressure in the tank. Thus there was not enough usage of the hydrogen compared to the one stored. That is normal because the tank was chosen to store very highly compressed hydrogen.

5.2.3 – Summer day

As with the two previous scenarios, first the power produced by the PV generator is presented in Figure 5.20:

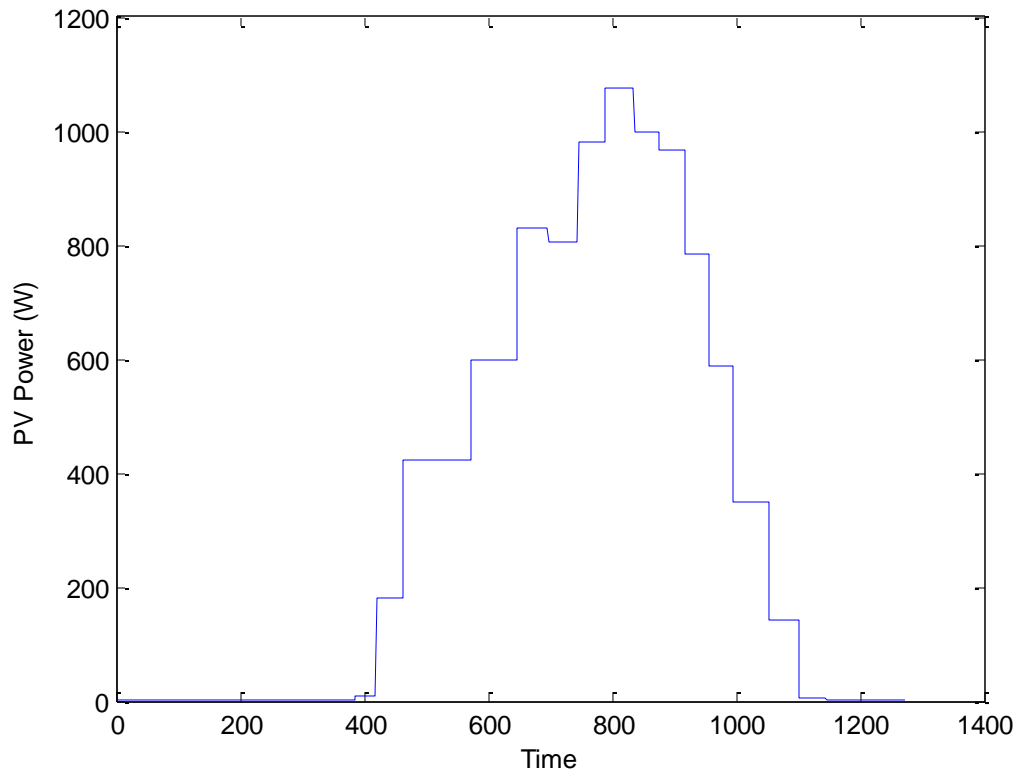


Figure 5.20: PV power for 1st of July

Looking back at the previous scenario, the power generated by the PV during the spring day is more than the one at the summer day. This is normal, as, according to the data, there was more irradiation during the spring day. The temperature is higher in the summer but it is obvious and expected that the irradiation is more important to the PV power generation.

In Figure 5.21 the plot of the PV power and the Load is shown:

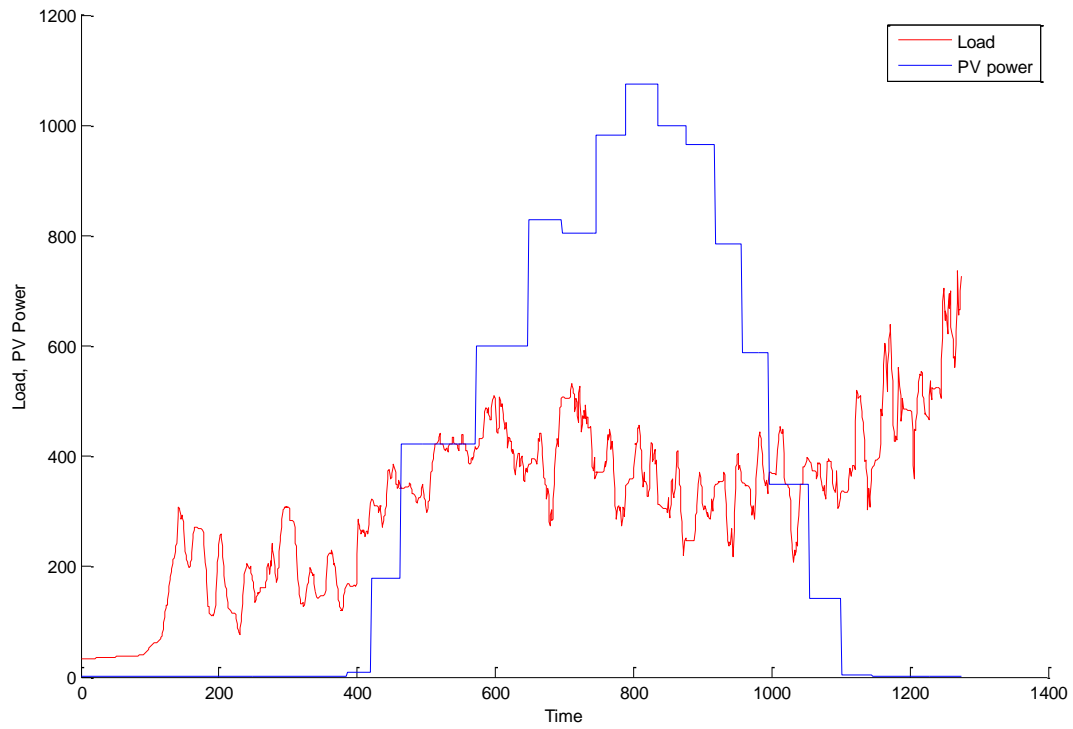


Figure 5.21: PV power and Load for 1st of July

Again the PV power generation during the day is enough to cover the power shortage during night hours. This is better shown in Figure 5.22:

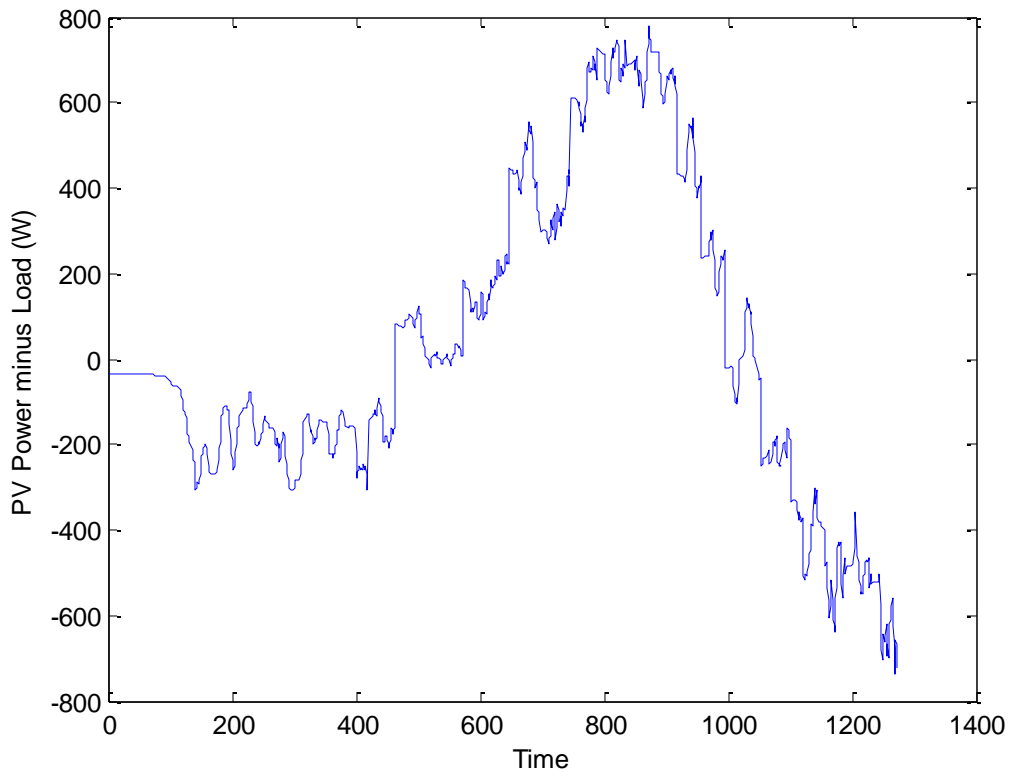


Figure 5.22: Difference between PV power and Load for 1st of July

The relationship between PV power, FC power and Load is shown in Figure 5.23:

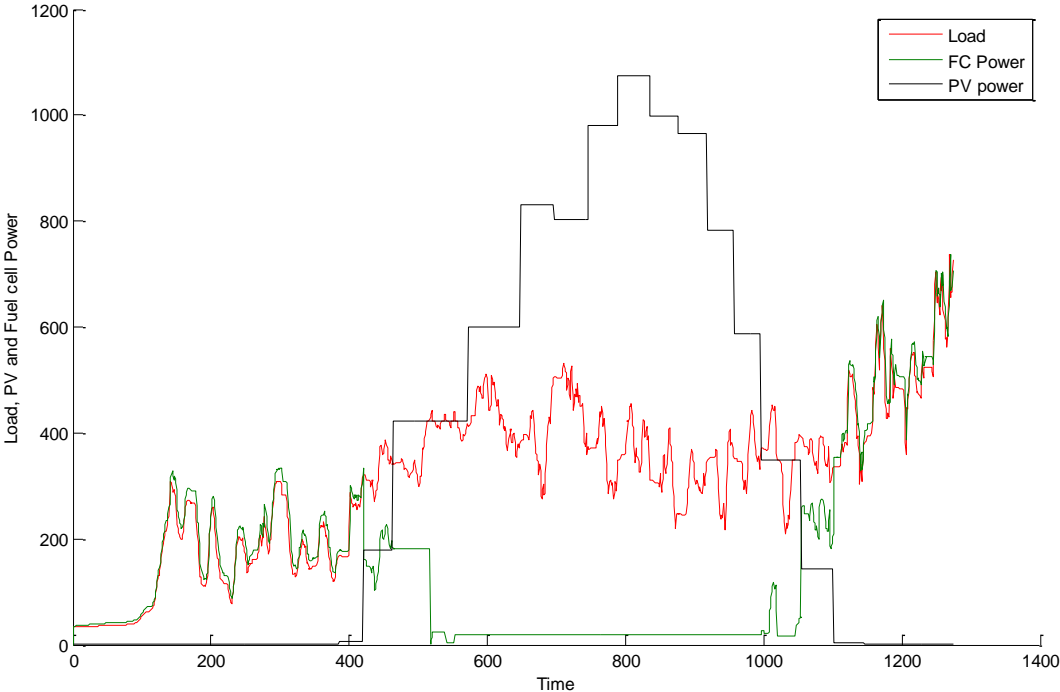


Figure 5.23: PV and FC power and Load for 1st of July

In the two final graphs of this section, Figure 5.24 and 5.25, the behavior of the battery and the hydrogen tank are shown respectively with the same observations as in the spring scenario:

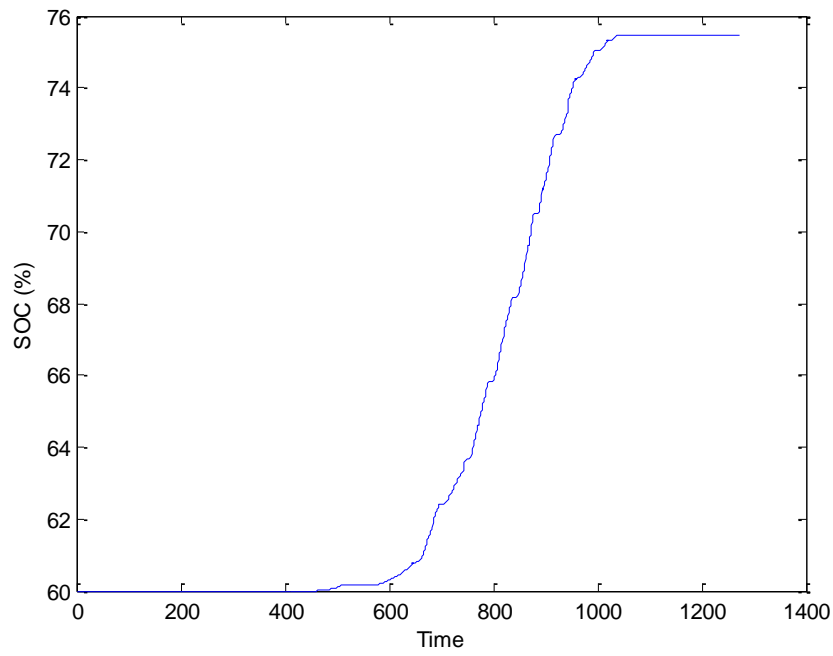


Figure 5.24: SOC at 1st of July

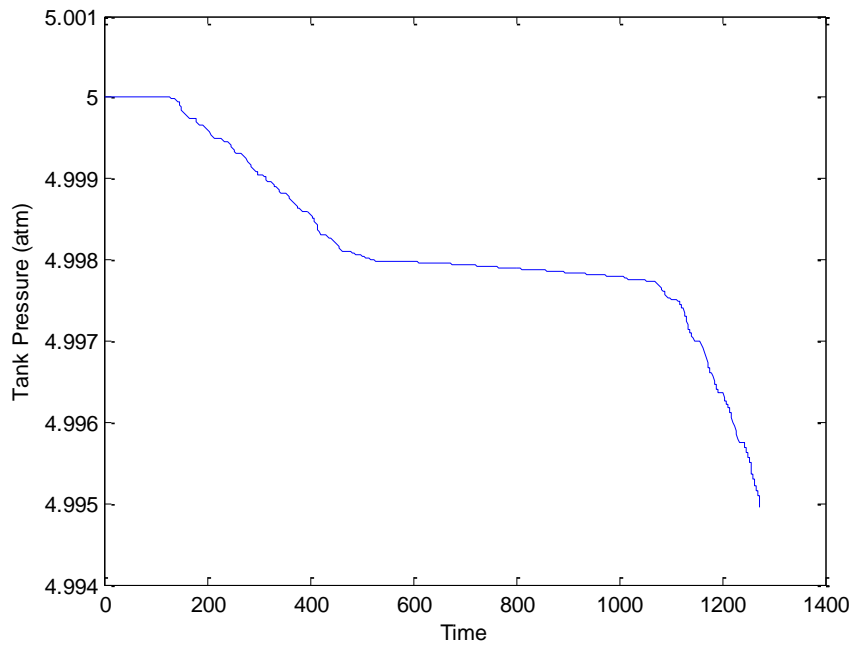


Figure 5.25: Tank pressure at 1st of July

5.2.4 – Special cases

First the behavior of the electrolyser is examined if the battery is full. The result is shown in Figure 5.26:

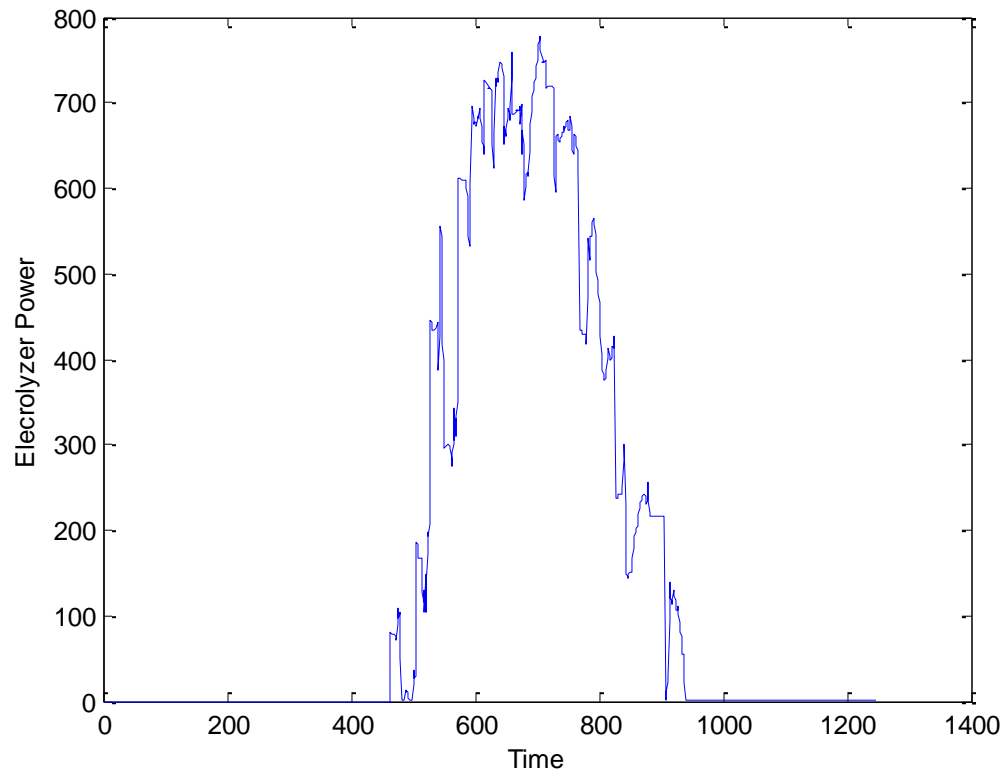


Figure 5.26: Electrolyser at work

We can see that the electrolyzer converts power during the day hours, when there is power surplus. This power is converted to hydrogen in the hydrogen Tank, as shown in Figure 5.27:

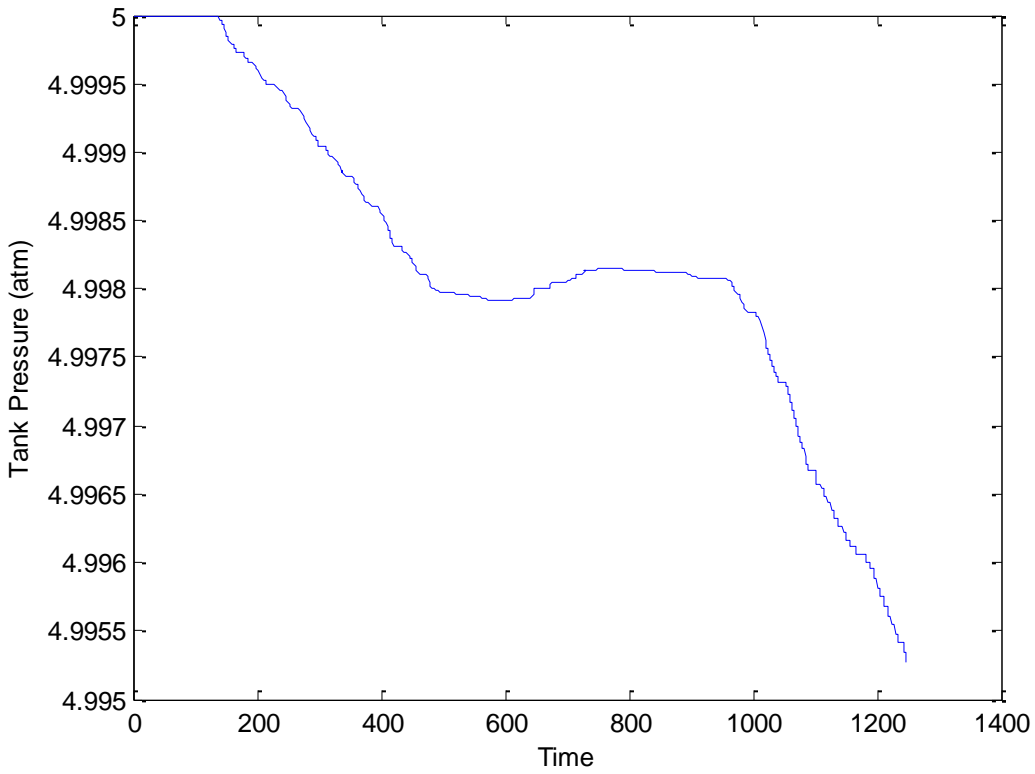


Figure 5.27: Tank pressure in electrolyser usage case

It is obvious that the pressure increases during daytime, when the electrolyser is at work.

If the pressure of the tank is set to full then in Figure 5.28 is shown that the power surplus has to be dumped as excess power:

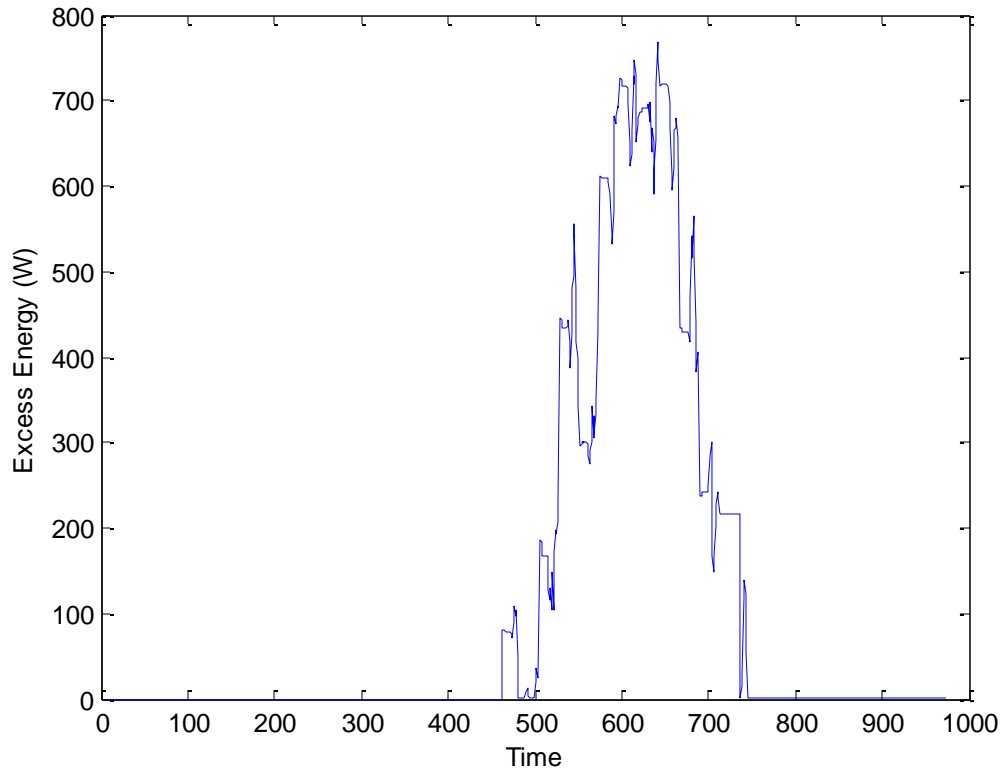


Figure 5.28: Excess Power

The last special case examined is when the load is extreme and the system has to come to a halt. In Figure 5.29 it can be seen that after a certain point the PV generator, in co-ordination with the fuel cell stack cannot produce the necessary power to meet the needs of the system. The battery is set to be empty and the result is that the emergency signal kicks in, as shown in Figure 5.30.

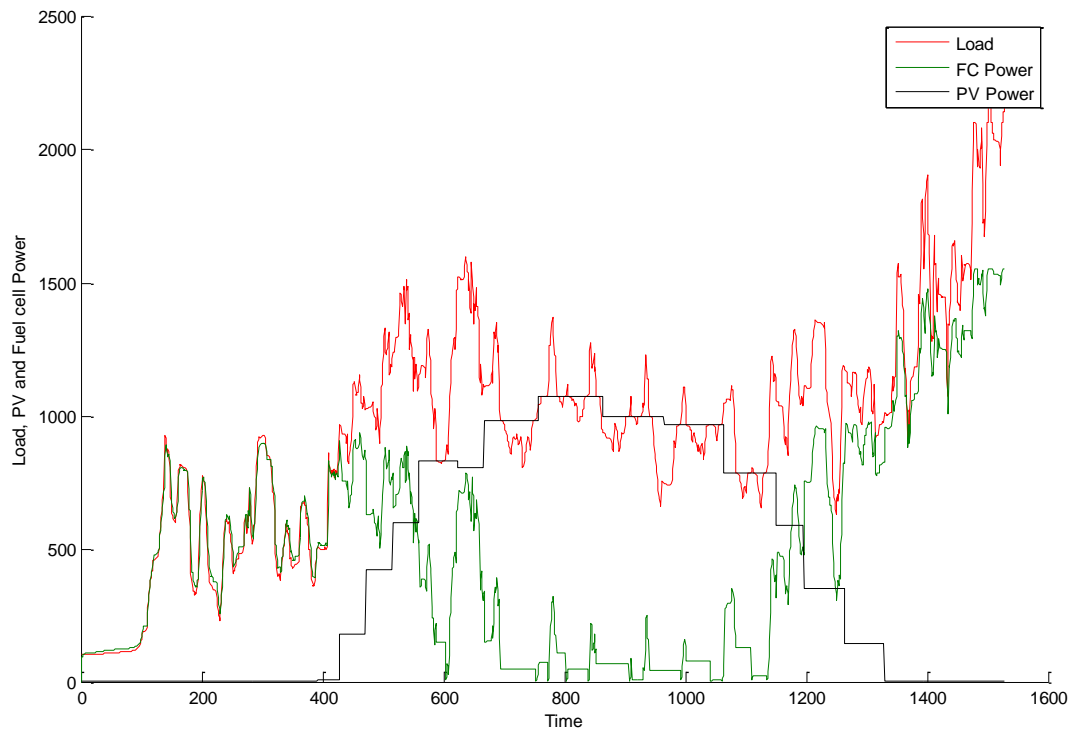


Figure 5.29: PV and FC power – Excessive Load

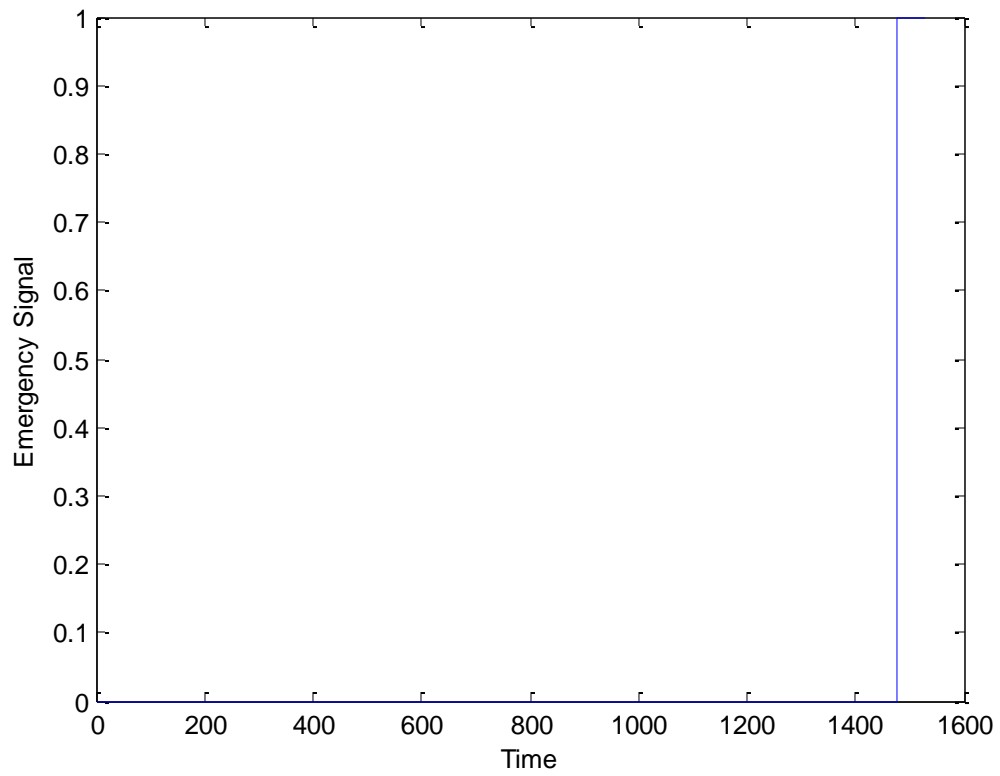


Figure 5.30: Emergency signal operating

The final conclusions of the simulation will be given in the following chapter.

Chapter 6 – Conclusions and recommendations

In this work a complete model for a hydrogen PVFC hybrid system has been implemented in Simulink and utilized to predict its operational performance through dynamic simulation.

6.1 – Modeling of PVFC hybrid system components

Detailed descriptions of the individual component models required to simulate a hydrogen PVFC hybrid system are presented. These models are mainly based on electrical and electrochemical relations. However, a number of empirical relationships for some models are used. The models of the PV generator and Fuel cell stack are discussed in detail, while the electrolyser and the hydrogen storage tank are represented by simple models. The controller is given by a flow diagram as its Simulink implementation shows no particular interest because it consists mainly of if action blocks.

6.1.1 – PV Generator

Two PV generator models are discussed in this work: the one-diode model and the two-diode model. The second model was chosen for this system, as it is more corresponding to the physical properties of the PV generator.

6.1.2 – Hydrogen energy system

The PEM fuel cell is modeled by using analytical equations, but it also includes some empirical aspects (i.e. internal resistance), when the theoretical analysis is too complicated or the parameters are not accessible.

6.1.3 – Overall Operation of hydrogen PVFC system

The main conclusion drawn from the simulation of the system is that the model corresponds well to the performance of an actual system. The results of the simulation have shown that the operational performance of the system does not depend only on component efficiencies, but also on system design and consumption behavior. The sizing of the system was not optimum, as the simulation for the summer day showed that maybe it does not store a significant amount of energy during the summer. But the PV generator unit chosen has a size of 1 square meter, so adding one or two more PV modules is easy.

6.2 – Recommendations for future work

- Adding other renewable resources to the system, such as a wind turbine, to the system. A wind energy conversion would reduce the required PV generator area and reduce the hydrogen storage volume. A trade-off between PV generator area and wind generator size is an interesting challenge for systems located at sites with high wind speeds.
- Adding a MPP tracker to the system in order to optimize the PV generator performance

- Trying different fuel cells, instead of the PEM fuel cell. SOFC is a very attractive option for cooperation with a CHP machine, as it operates at very high temperatures, producing useful energy in the form of heat.

CHAPTER 7 – References

- [1]: T. Veziroglu: Hydrogen Energy System: A Permanent Solution to Global Problems, Clean Energy Research Institute, USA, Web Site, visit 2004.
- [2]: Abou El-Maaty Metwally Metwally Aly Abd El-Aal From Ain Shams University/Egypt, Modeling and Simulation of a Photovoltaic Fuel Cell Hybrid System, 2006
- [3]: S. Krauter and R. Araujo: New Power Conditioning Unit Incorporating Charge Controller, Energy Flow Monitor, Data Logger, DC/AC Converter for Stand Alone and Combined PV-Diesel Operation, Proc. 16th EPVSEC, Glasgow, UK, 2000, pp. 2575-2577.
- [4]: P. Hollmuller, J. Joubert, B. Lachal, and K. Yvon: Evaluation of a 5 kWp Photovoltaic Hydrogen Production and Storage Installation for a Residential Home in Switzerland, International Journal of Hydrogen Energy 25, 2000, pp. 97-109.
- [5]: M. Almonacid and J. Aguilera: Fuzzy Logic Charge Regulator, 2nd World Conference And Exhibition on PV Solar Energy Conversion, Vienna, Austria, 1998, pp. 32733275.
- [6]: G. Hoogers: Fuel Cell Technology handbook, CRC press LLC, 2003.
- [7]: Winfried Hoffmann: PV Solar Electricity: One Among the New Millennium Industries, 17th EPVSEC, Paper No. PB 2.1, Munich, Germany, 2001, pp. 851-861.
- [8]: Bryan Fry: Simulation of Grid-Tied Building Integrated Photovoltaic Systems, M.Sc., University of Wisconsin, Madison, 1998.
- [9]: Oystein Ulleberg: Stand-alone power systems for the future: optimal design, operation & control of Solar-Hydrogen energy systems, Ph.D. dissertation, Norwegian University, Trondheim, 1998.
- [10]: Franz Kininger: Photovoltaic Systems Technology, Rationelle Energiewandlung, Universistät Kassel, Deutschland, 2003.
- [11]: Rejane Moraes-Duzat: Analytical and Experimental Investigation of Photovoltaic Pumping Systems, Ph.D. dissertation, University Oldenbury, Germany, 2000.
- [12]: G. E. Ahmad, M. A. Mohamad, S. A. Kandil, and R. Hanitsch: Fault Detection in PV Generators Using an Improved Electronic Load, 14th EPVSEC, Barcelona, Spain, 1997, pp. 199-202.
- [13]: Yeong-Chau Kuo and Tsorng-Juu Liang: Novel Maximum-Power-Point-Tracking Controller for Photovoltaic Energy Conversion System, IEEE transactions on industrial electronics, Vol. 48, No. 3, 2001, pp. 594-601.

- [14]: M. Jantsch, M. Real, H. Häberlin, C. Whitaker, K. Kurokawa, G. Blässer, P. Kremer, and C. W. G. Verhoeve: Measurement of PV Maximum Power Point Tracking Performance, 14th EPVSEC, Barcelona, Spain, 1997, pp. 2188-2193.
- [15]: T. Hottinen: Technical Review and Economic Aspects of Hydrogen Storage Technologies, MSc, Helsinki University of Technology, Department of Engineering Physics and Mathematics, Espoo, 2001.
- [16]: Dr. Joan M. Ogden: Review of Small Stationary Reformers for Hydrogen Production, a report for International Energy Agency (IEA) agreement on the production and utilization of Hydrogen, Princeton University, 2002.
- [17]: R. Bafna, J. Beulow, and et al: *Transition to a Hydrogen-Based Energy Systems: The next Ten Years*, Conferences-Reinforcement Papers, Toronto, Canada, 2002.
- [18]: Web Site, Quantum Technologies, Inc., Visit 2003. <http://www.qttw.com>
- [19]: VLEEM: Final report: Very Long Term Energy Environment Modelling, 2002.
<http://www.vleem.org/PDF/annex8-monograph-distribution.pdf>
- [20]: C. Möller and R. Lucks: Seminar: Fuel Cells, Technical faculty, University of Kiel, Germany, 2000.
<http://www.texnic.de/FC/>
- [21]: F. Barbir: *Review of Hydrogen Conversion Technologies*, Clean Energy Research Institute, University of Miami, Coral Gables, FL 33124, U.S.A, Visit 2003.
<http://www.iahi.org/H2Convrt.doc>
- [22]: M. Noponen: Experimental Studies and Simulations on Proton Exchange Membrane Fuel Cell Based Energy Storage Systems, MSc, Helsinki University of Technology, Department of Engineering Physics and Mathematics, Espoo, 2000.
- [23]: Messenger, Roger & Jerry Ventre, *Photovoltaic systems engineering 2nd Edition*, CRC Press, 2003
- [24]: Castanes, Luis & Santiago Silvestre, *Modeling Photovoltaic Systems Using Pspice*, John Wiley & Sons Ltd, 2002
- [25]: Walker, Geoff R. , *Evaluating MPPT converter topologies using a Matlab PV model*, Australian Universities Power Engineering Conference, Brisbane 2000

Appendix

Table of figures

2.1: Concept of a PVFC hybrid system.....	12
2.2: I-V curves for an electrolyser cell for low and high temperatures.....	16
2.3: Control strategy diagram.....	20
3.1: One-diode model.....	22
3.2: Short-circuit and open circuit conditions.....	22
3.3: Two-diode model.....	24
3.4: Equivalent circuit used.....	25
3.5: PV subsystem.....	29
3.6: PV power for one PV module at the first week of winter.....	30
3.7: Operation of a PV module with varied temperature.....	31
3.8: Simulink model for a single PV cell.....	32
3.9: Simulink model for calculation of short-circuit current.....	33
3.10: Simulink model for calculation of reverse saturation current.....	33
3.11: Simulink model for calculation of thermal potential.....	34
4.1: A single PEM fuel cell configuration.....	36
4.2: PEMFC assembly.....	42
4.3: The structure for carbon supported catalyst.....	43
4.4: Fuel cell inputs and outputs.....	44
4.5: Voltage/current density graph for a low temperature fuel cell.....	49
4.6: Fuel cell subsystem.....	52
4.7: Fuel cell stack.....	53
4.8: Fuel cell.....	54

4.9: Hydrogen pressure.....	55
4.10: Pressure of oxygen.....	56
4.11: Pressure of water.....	57
4.12: Nernst equation.....	58
4.13: Activation losses.....	59
4.14: Faraday’s law.....	61
4.15: Faraday’s efficiency.....	61
4.16: Tank.....	62
5.1: 1 st of January – Temperature.....	63
5.2: 1 st of January – Irradiation.....	64
5.3: Load for one household for one day.....	64
5.4: 1 st of April – Temperature.....	65
5.5: 1 st of April – Irradiation.....	65
5.6: 1 st of July – Temperature.....	66
5.7: 1 st of July – Irradiation.....	66
5.8: PV generator power for a winter day.....	67
5.9: PV power and Load for 1 st of January.....	68
5.10: Difference between PV power and Load.....	69
5.11: FC power, PV power and Load.....	70
5.12: SOC for 1 st of January.....	71
5.13: 1 st of January – Tank pressure.....	71
5.14: PV power for 1 st of April.....	72
5.15: PV power and Load for 1 st of April.....	73
5.16: Difference between Load and PV power for 1 st of April.....	74
5.17: FC power, PV power and Load.....	75

5.18: SOC for 1 st of April.....	76
5.19: Tank pressure for 1 st of April.....	77
5.20: PV power for 1 st of July.....	78
5.21: PV power and Load for 1 st of July.....	79
5.22: Difference between PV power and Load for 1 st of July.....	80
5.23: FC power, PV power and Load.....	81
5.24: SOC for 1 st of July.....	82
5.25: Tank pressure for 1 st of July.....	82
5.26: Electrolyser at work.....	83
5.27: Tank pressure in electrolyser usage case.....	84
5.28: Excess power.....	85
5.29: PV and FC power – Excessive Load.....	86
5.30: Emergency signal operating.....	87

List of Tables

2.1: Band gap, maximum current density, and theoretical efficiency of some different semiconductor technologies.....	13
3.1: Datasheet for the PV module.....	29
4.1: Basic fuel cell components.....	37
4.2: Data for different types of fuel cells.....	38
4.3: ΔG_f for the basic reaction in a hydrogen fuel cell.....	45
4.4: ΔG_f , EMF and efficiency limits for hydrogen fuel cell.....	47
4.5: i_0 for several electrode materials for acid electrolyte.....	50

Matlab code for estimation of PV current

Matlab code for estimation of formula 3-21:

```
function Icell = Current(Iph, Ir, Vc, Vt_Ta)

Rs = 5.1*10^(-3);      %% Rs = 5.1;

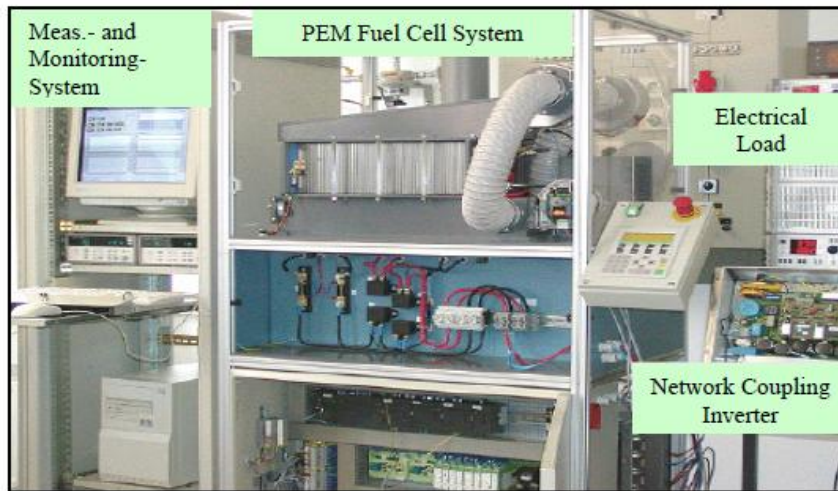
Ia=zeros(size(Vc)); % Initialize Ia with zeros
% Perform 5 iterations
for j=1:5;
    Ia = Ia - (Iph - Ia - Ir .* ( exp((Vc + Ia .* Rs) ./ Vt_Ta) -1))...
        ./ (-1 - Ir * (Rs ./ Vt_Ta) .* exp((Vc + Ia .* Rs) ./ Vt_Ta));
end

Icell = Ia;
```

This is the embedded Matlab code used to calculate, with satisfying accuracy, the current of the PV module. The accuracy is guaranteed by the fact that 5 iterations are used for the estimation of the current.

Datasheet for fuel cell unit

Power Data	
Electrical rated power	2kW (2 × 1kW)
Maximum electric power	3kW (2 × 1.5kW)
Open circuit voltage	2 × ca. 48V
Rated electric current	34A
Rated electric voltage	30V
Maximum electric current per stack	60A
Hydrogen consumption at rated electric power	Ca. 1.6Nm ³ /h (every stack 0.8Nm ³ /h)
CHP coefficient at operating point	0.92
Power peripheral supply	Max. 10A at 24V _{DC}
Fuel Gas Supply	
Operating pressure of hydrogen	20 – 40kPa
Maximum operating pressure of hydrogen	50kPa
Connection pressure of hydrogen	500kPa
Tube/flexible tube diameter for hydrogen supply	High-grade steel, outside diameter 10mm
Hydrogen loss through sink cycle	40kPa per purge (0.3s) ca. 570ml
Dimensions	
Width × depth × high	110cm × 70cm × 172cm
Environmental Conditions	
Permissible ambient temperature	15 to 25°C
Permissible relative humidity	30 to 70%



2kW PEM fuel cell system in ISET (KASSEL, Germany)

This fuel cell unit was used as a model for the system under study, with the difference that only one stack was used instead of the two in this configuration.